Manipulation of superparamagnetic beads on patterned Au/Co/Au multilayers with perpendicular magnetic anisotropy

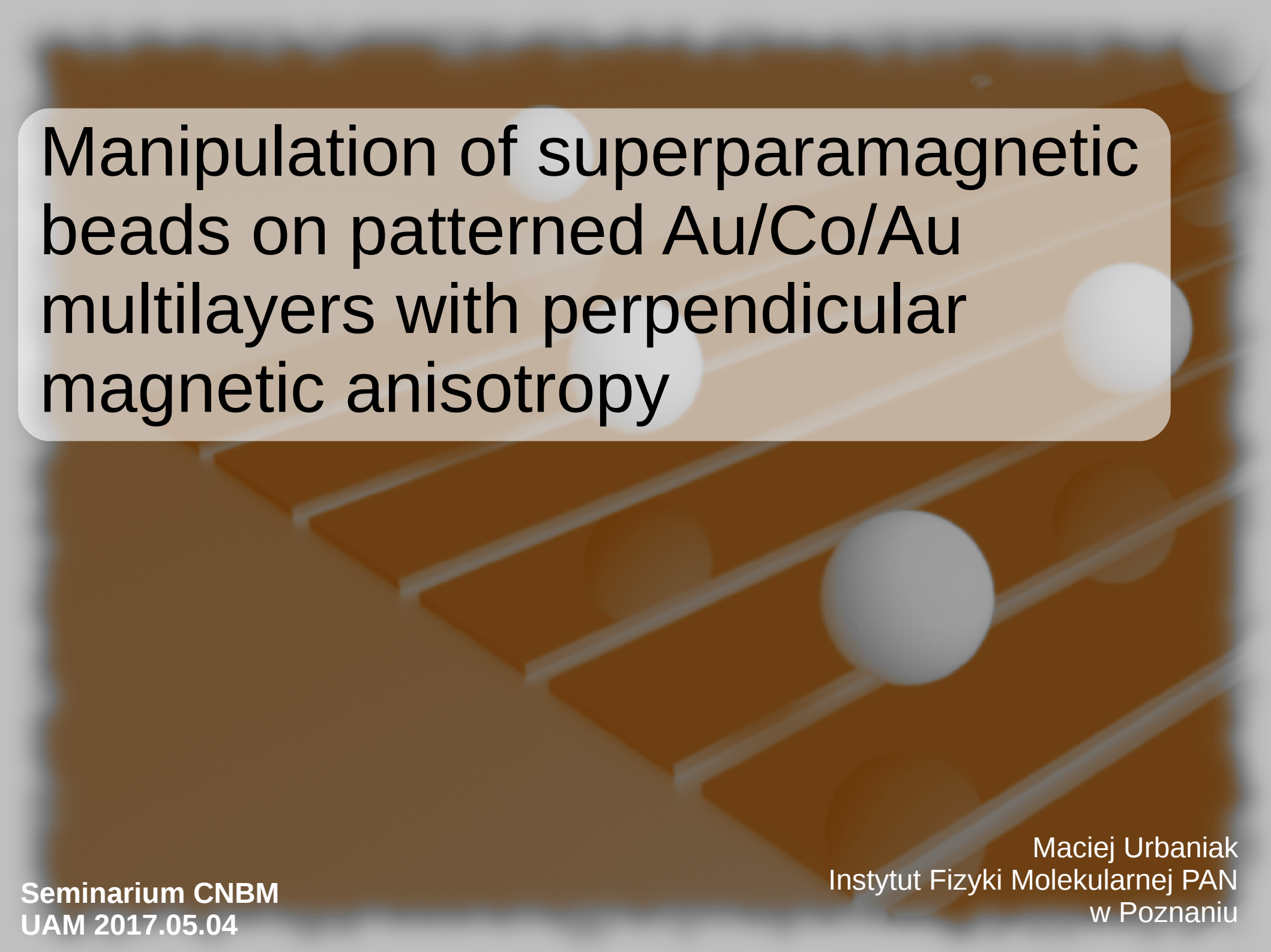

Maciej Urbaniak
Instytut Fizyki Molekularnej PAN
w Poznaniu

Seminarium CNBM
UAM 2017.05.04

Manipulation of superparamagnetic beads on patterned Au/Co/Au multilayers with perpendicular magnetic anisotropy

- Motivation
- Literature examples
- Forces in magnetic field
- Perpendicular magnetic anisotropy in thin Au/Co/Au films
- Magnetic fields over patterned magnetic films
- Magnetophoresis

Manipulation of superparamagnetic beads on patterned Au/Co/Au multilayers with perpendicular magnetic anisotropy

The work was financed by the National Science Center Poland (**NCN**) under HARMONIA funding scheme for international research projects - decision No. DEC-2013/08/M/ST3/00960

- Motivation
- Literature examples

Ferromagnetyczne materiały dla kontrolowanego pozycjonowania ścian domenowych

- Forces in magnetic field
- Perpendicular magnetic anisotropy in thin Au/Co/Au films
- Magnetic fields over patterned magnetic films
- Magnetophoresis

A. Jarosz, D. Holzinger, M. Urbaniak, A. Ehresmann, F. Stobiecki
Manipulation of superparamagnetic beads on patterned Au/Co/Au multilayers with perpendicular magnetic anisotropy
J. Appl. Phys. **120**, 084506 (2016)

FACT:

- steadily increasing volume of business and tourist travel

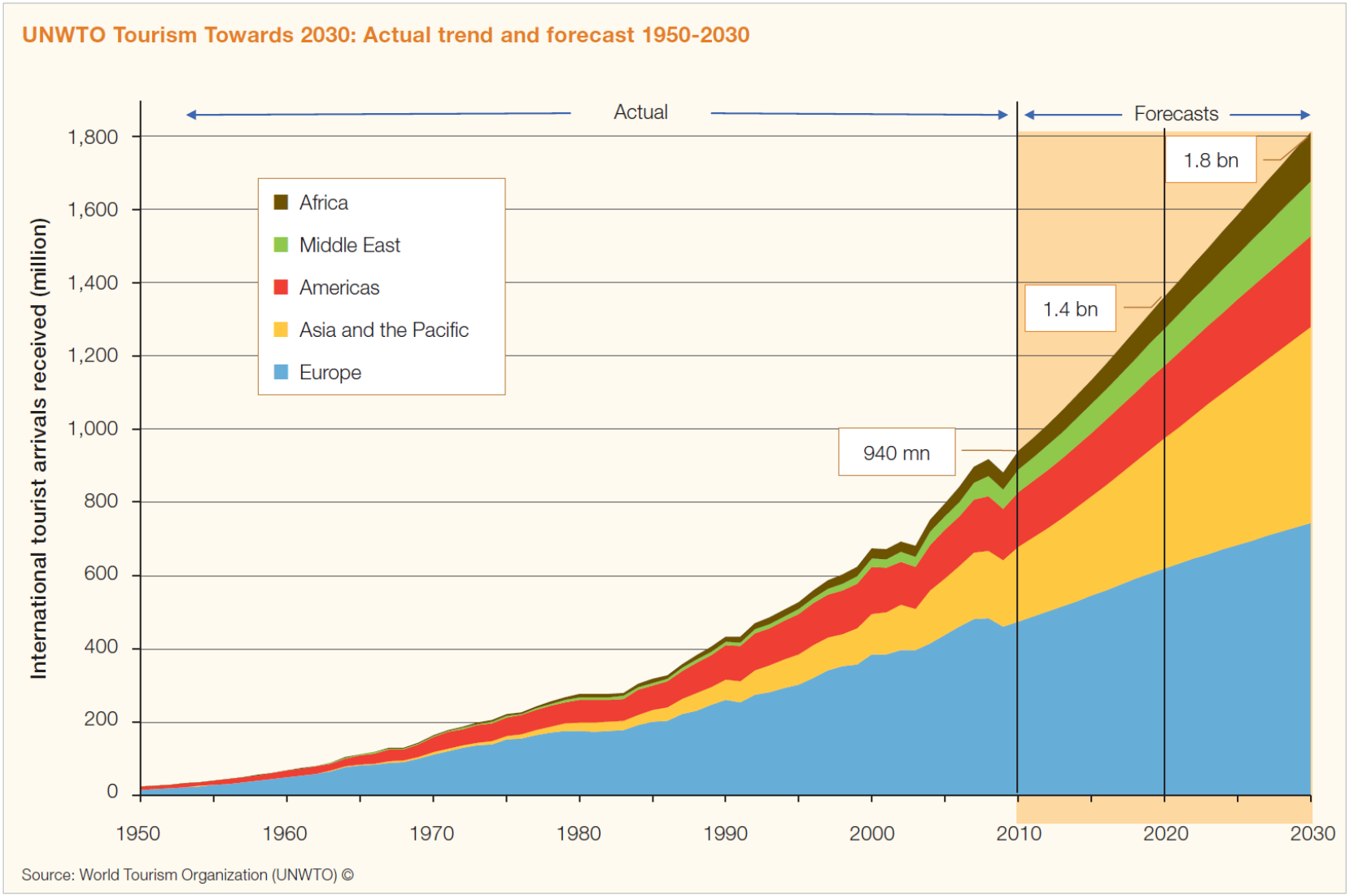

FACT:

- steadily increasing volume of business and tourist travel

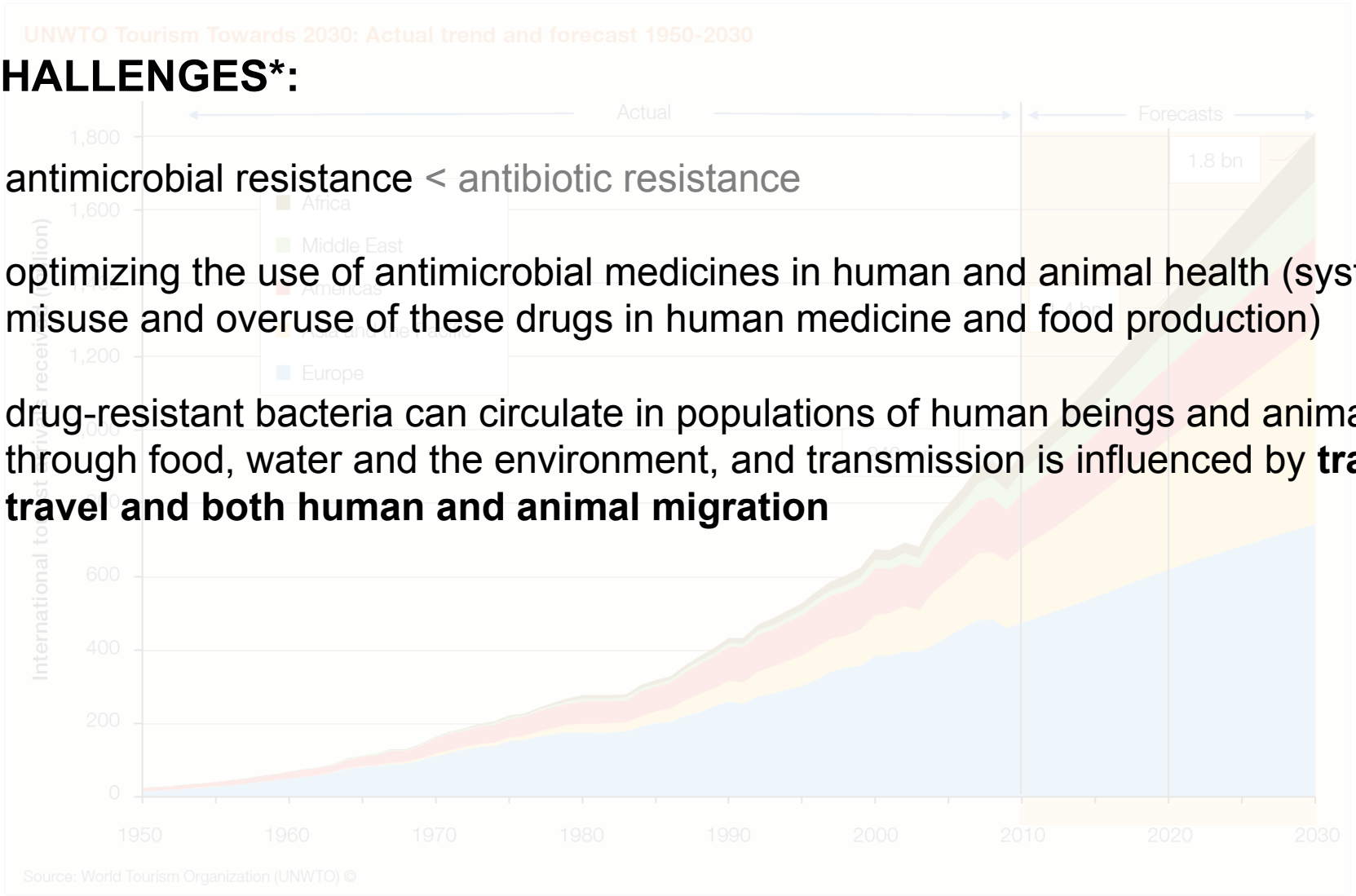

CHALLENGES*:

- antimicrobial resistance < antibiotic resistance
- optimizing the use of antimicrobial medicines in human and animal health (systematic misuse and overuse of these drugs in human medicine and food production)
- drug-resistant bacteria can circulate in populations of human beings and animals, through food, water and the environment, and transmission is influenced by **trade, travel and both human and animal migration**

* WHO, Global Action Plan On Antimicrobial Resistance

SOLUTIONS:

- ”big” danger

Juan Carlos Alfonso Víctor María de Borbón y Borbón-Dos Sicilias

former honorary president of WWF Fund Spain

El Rey que cazaba elefantes

The image removed due to copyrights concerns.
In the original presentation shown here was a photograph of two hunters with a killed elephant in the background.
http://www.elmundo.es/ciencia/2014/06/02/538c6070ca4741ea2a8b4572.html

image from 2006, Botswana

SOLUTIONS:

WHO, Global Action Plan On Antimicrobial Resistance

*Antibiotics must also be supplemented by **affordable**, point-of-care diagnostic tools to inform health practitioners and veterinarians of the susceptibility of the pathogens to available antibiotics. The applicability and affordability of these techniques in **low- and middle-income countries** must be considered.*

Lab-on-a-chip device

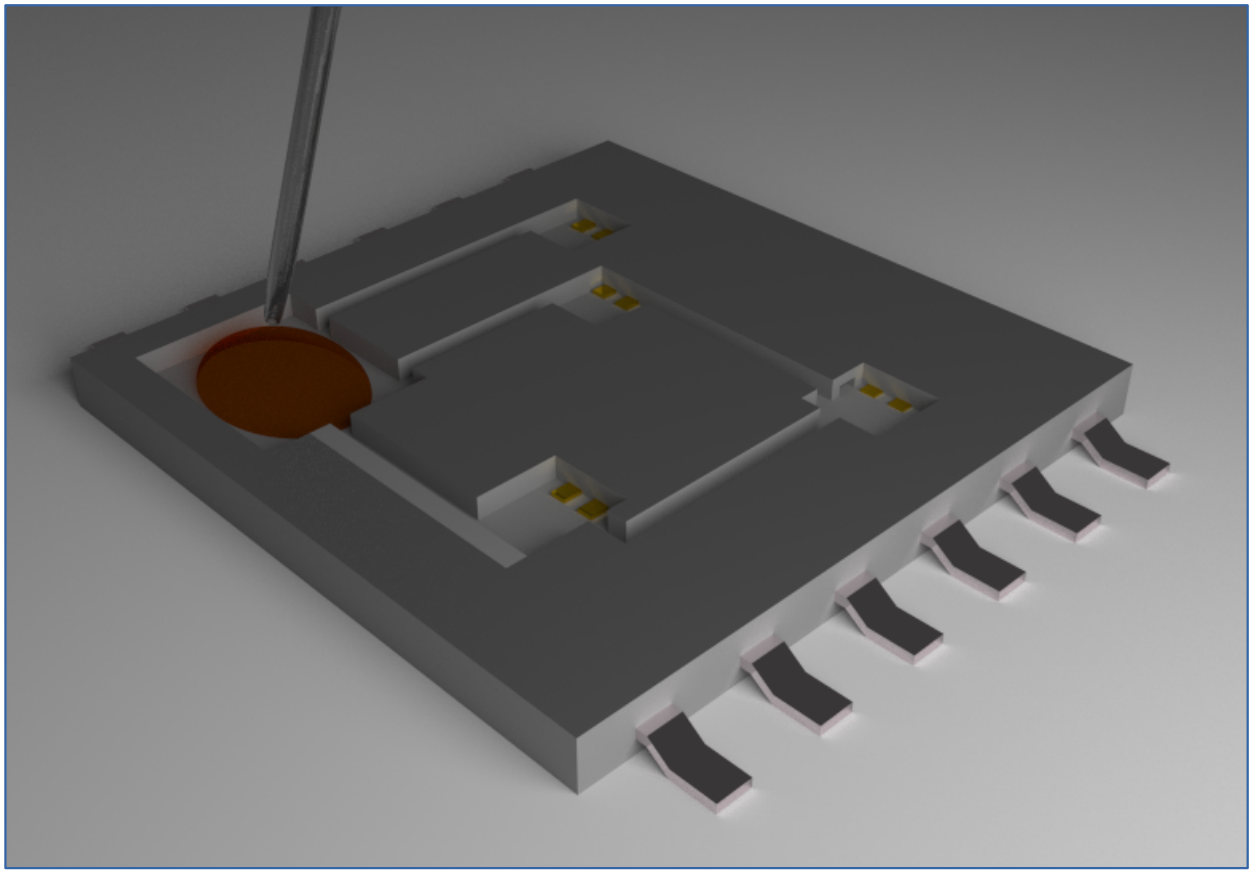

the need to transport magnetic beads in fluidic channels

SOLUTIONS:

WHO, Global Action Plan On Antimicrobial Resistance

*Antibiotics must also be supplemented by **affordable**, point-of-care diagnostic tools to inform health practitioners and veterinarians of the susceptibility of the pathogens to available antibiotics. The applicability and affordability of these techniques in **low- and middle-income countries** must be considered.*

Lab-on-a-chip device

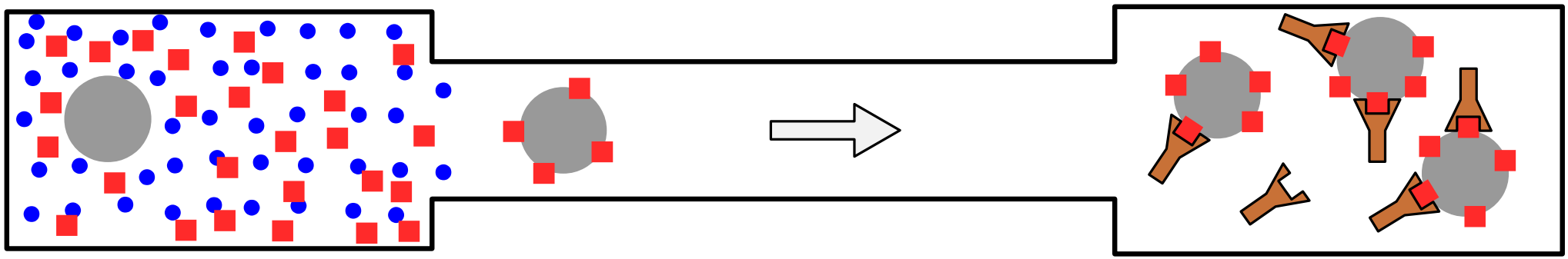

the need to transport magnetic beads in fluidic channels

Separation from bulk solution

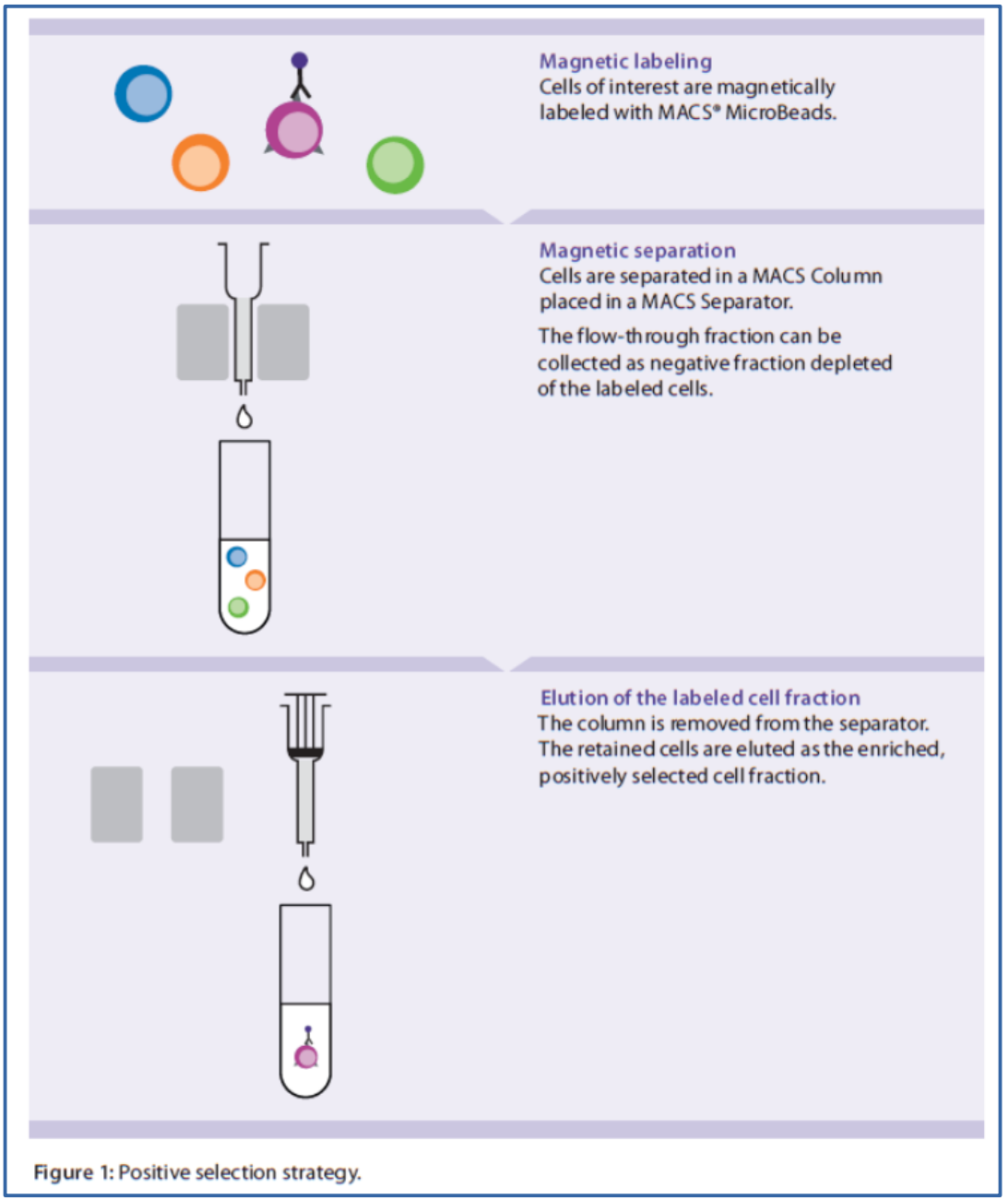

Figure 1: Positive selection strategy.

Magnetic particles are functionalized to bind to specific cells or other chamicals

Miltenyi_Biotec_Catalog2009.pdf, www.miltenyibiotec.com

Typical manipulation procedures

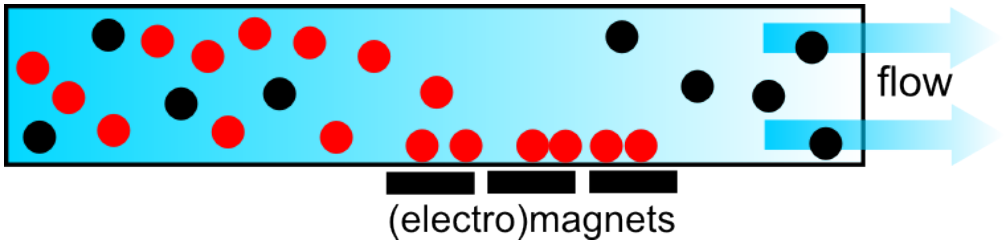

Magnetic particles captured - **separation**

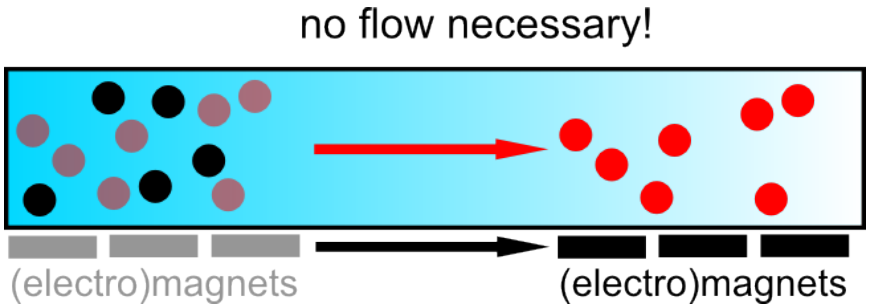

Magnetic particles moved - **transport**

Magnetophoresis - motion induced by a magnetic field on a particle of magnetic material in a fluid. [en.wiktionary.org]

Electrophoresis – used in forensic DNA analysis

[1] Martin A. M. Gijs, Frédéric Lacharme, and Ulrike Lehmann, Chamical Reviews **110**, 1518 (2010)

Even more typical manipulation procedures

35 t

www.ainsmag.co.uk/newsimages/st165/4067st2h.jpg

Magnetic beads

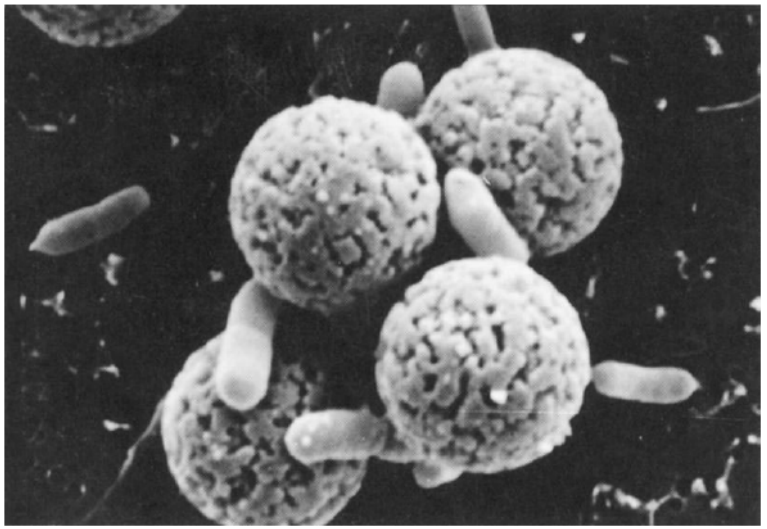

Fig. 2. An electron micrograph showing *E. coli* O157 bound to Dynabeads. Reproduced, with permission, from materials provided by Dynal, Oslo, Norway.

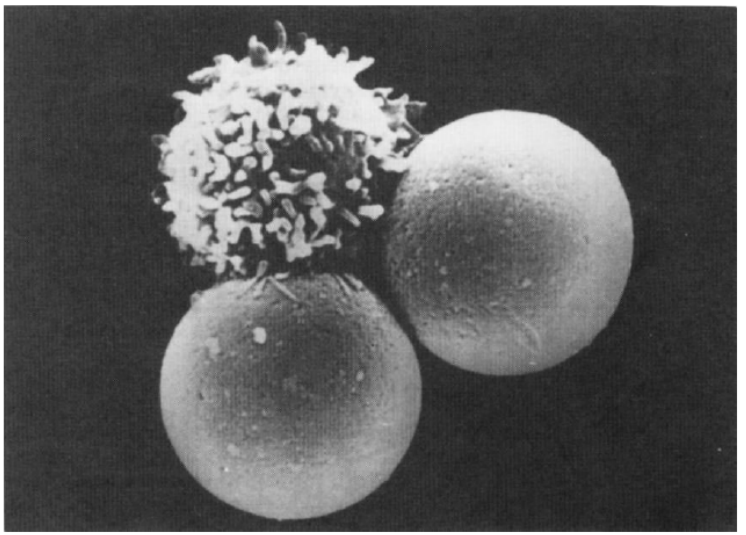

Fig. 3. An electron micrograph showing a T-lymphocyte bound to two Dynabeads M-450. Reproduced, with permission, from Ref. [8].

Diameters – several µm (Dynabeads M-270 D=2.8 µm)
Magnetic core – iron oxides
Susceptibility, χ=0.17 (Dynabeads M-270)

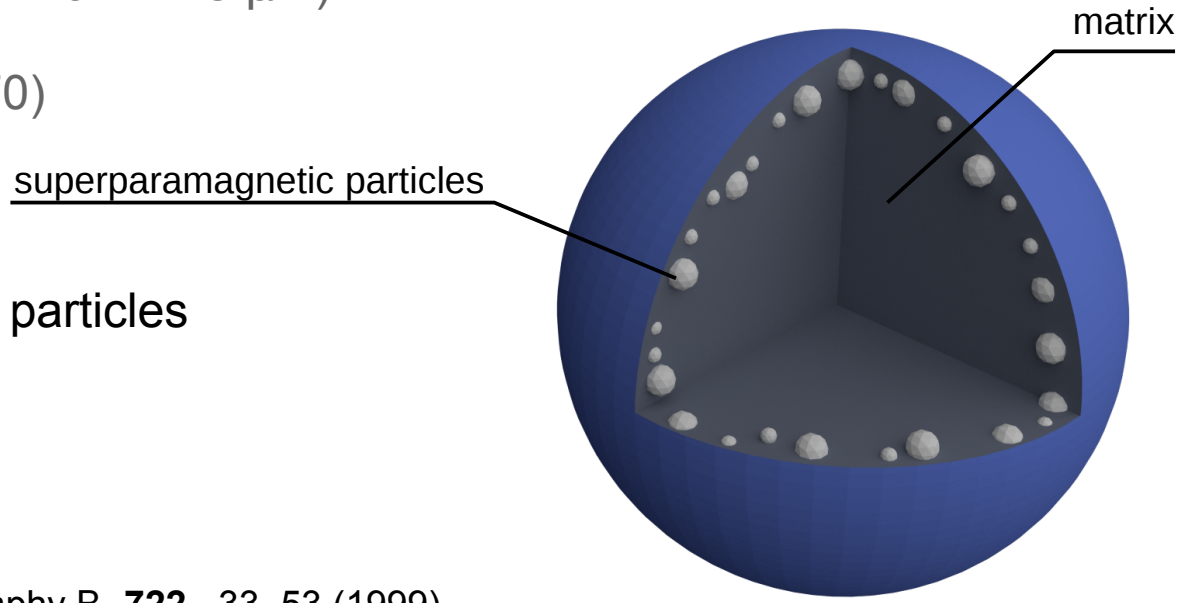

Micromod – 4 µm diameter
100nm thick layer of superparamagnetic particles
10 nm beneath the outer functionalized surface

[11] I. Šafařik, M. Šafařıková, Journal of Chromatography B, **722**, 33–53 (1999)

Superparamagnetic particles

- As a result of high moments the assembly of superparamagnetic particles saturates in relatively weak external fields:

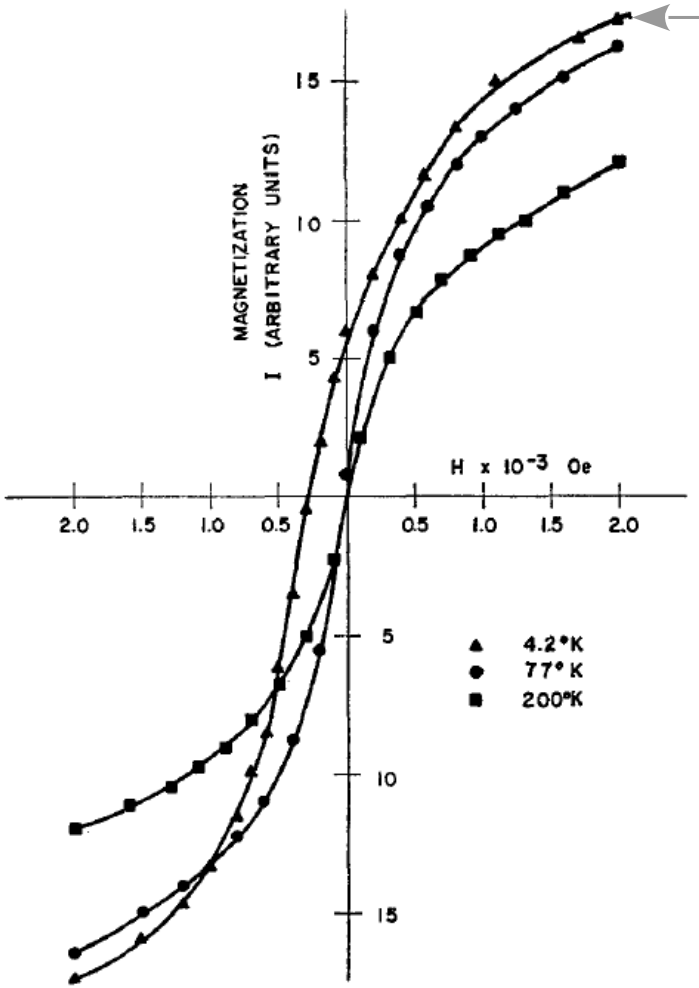

this curve is not "superparamagnetic"

FIG. 1. Low field portion of demagnetization curves of fresh iron amalgam. This amalgam consists of 2% iron by volume in the form of small iron particles whose diameters are estimated to lie between 30 A and 45 A.

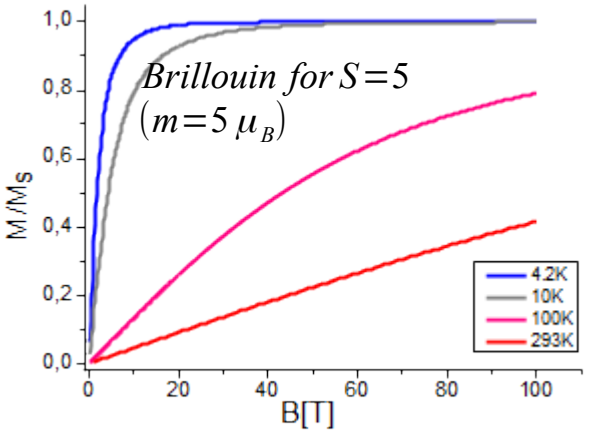

$$\frac{\langle S_z \rangle}{S} = B_S\left(\frac{g\,\mu_B S\,B}{k_B T}\right)$$

- **Very high moments *S*** of superparamagnetic particles results in saturation in much weaker fields
- Technical saturation can be reached even at room temperature

$$B_S(x) = \frac{2S+1}{2S}\coth\left(\frac{2S+1}{2S}x\right) - \frac{1}{2S}\coth\left(\frac{x}{2S}\right)$$

C. P. Bean and I.S. Jacobs, J. Appl. Phys. **27**, 1448 (1956)

Superparamagnetic particles

- As seen on previous slide the superparamagnetism disappears below critical blocking temperature T_B.
- We assume that the external field magnetized the sample to initial magnetization $\boldsymbol{M}_i$ and was turned off at t=0 [5]. The magnetization will start do decrease with a rate depending on temperature and $\boldsymbol{M}_i$. The time dependence may be approximated by:

$$\frac{dM}{dt} = f_0 M e^{-KV/k_B T} \equiv \frac{M}{\tau} \qquad with \qquad \frac{1}{\tau} = f_0 e^{-KV/k_B T}, \quad f \approx 10^9 Hz$$ - frequency factor

- Integrating we get:

$$M_R = M_i e^{-t/\tau}$$

- The relaxation time is very strongly dependent on V and T:

Spherical Co particle	
6.8 nm diameter	9 nm diameter
τ=0.1 s	$\tau=3.3\times10^9$ s (100 years)

- The assembly of 9 nm particles is essentially stable with respect to magnetization at RT [5]

Superparamagnetic particles – blocking temperature

- The assembly of small particles of a constant size will have a stable magnetization (τ=100 s). For uniaxial particles and the same as above criterion of stability we have:

$$T_b = \frac{KV}{25 k_B}$$

- Schematic representation of the behavior of single domain particles versus temperature:

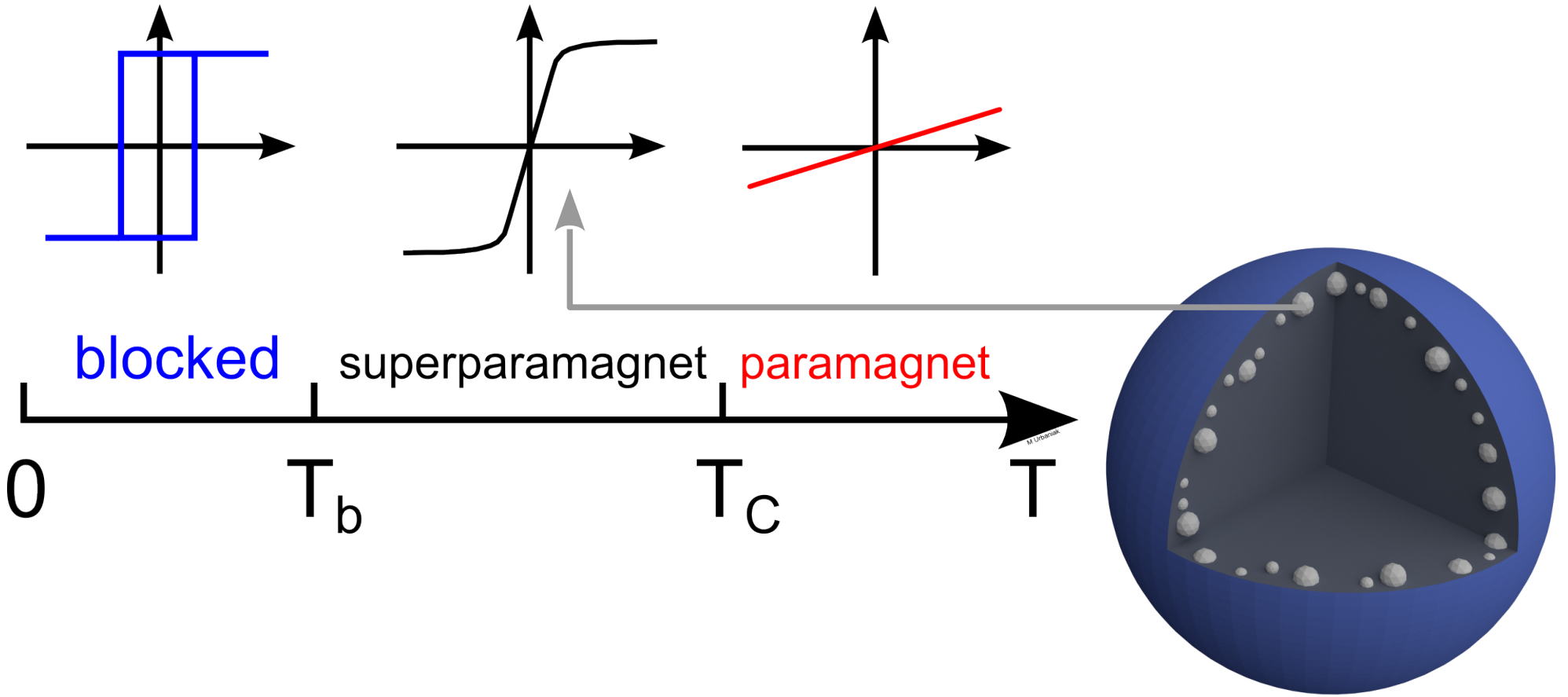

*graphics based on Fig.8.30 from J.M.D. Coey, Magnetism and Magnetic Materials, Cambridge University Press 2009

Forces in magnetic field

$\chi = \frac{\vec{M}}{\vec{H}} \rightarrow \chi_p = \frac{M}{H}$ $\qquad E = -\vec{m}\cdot\vec{B}$ $\qquad \vec{m} = \vec{M}\cdot V$ $\qquad V -$ volume of the magnet

- the induced magnetic moment of a superparamagnet is parallel to the external field
- we bring the magnet from infinity (B=0) to the location with the magnetic field B and decrease thus its energy:

$$m = V\chi_p \frac{B}{\mu_0} \rightarrow dm = V\chi_p \frac{dB}{\mu_0} \rightarrow dE = -dm\,B = -V\chi_p \frac{dB}{\mu_0} B$$

$$E = -\int_0^{B(\vec{r})} V\chi_p \frac{B}{\mu_0} dB = -\frac{1}{2\mu_0} V\chi_p B^2$$

The force acting on a magnet is $\vec{F} = -\nabla E$:

$$\vec{F} = \frac{1}{2\mu_0} V\chi_p \nabla B^2$$

The higher the gradient of B^2 the higher the force acting on a para/superparamagnetic material

The formula is true within the field range in which susceptibility is constant

Forces in magnetic field – force in medium with $\chi_{fluid} \neq 0$

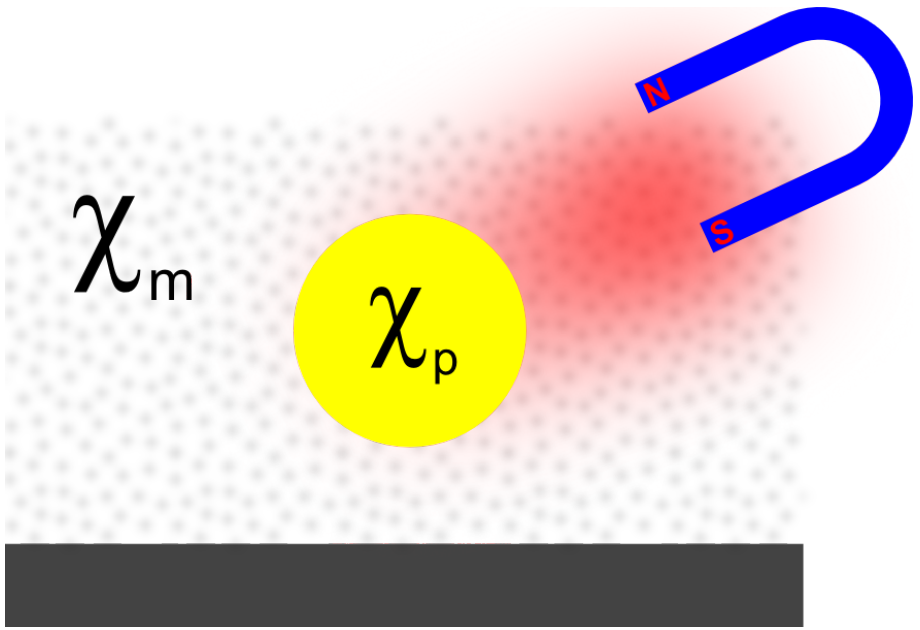

- because of biocompatibility most magnetophoresis experiments are performed in water or aqueous solutions
- the magnetic susceptibility of water is small ($\chi = \mathbf{-9.035 \times 10^{-6}}$) compared to susceptibility of typical magnetic bead ($\chi_p \sim \mathbf{0.1}$)
- D-glucose: $\chi = -10.92 \times 10^{-6}$

$$\vec{F} = \frac{1}{2\mu_0}(\chi_p - \chi_m) V \nabla(B^2) \approx \frac{1}{2\mu_0}\chi_p V \nabla(B^2)$$

χ_p, χ_m susceptibilities of particle and medium (e.g. water)

Nicole Pamme, Lab Chip, **6**, 24 (2006); P.W. Kuchel et al., Concepts in Magnetic Resonance Part A, **18A**, 56 (2003)

“Early days” of particle manipulation

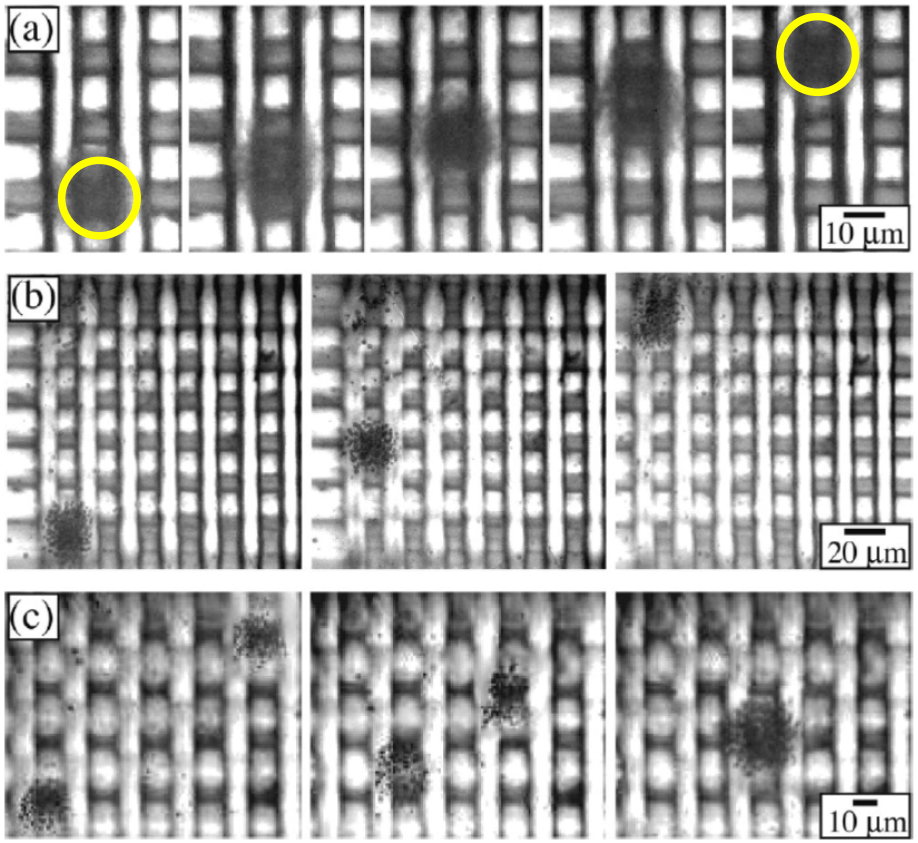

FIG. 4. (a) Demonstration of moving a group of superparamagnetic particles over two wires of a microelectromagnet matrix. The wire currents were adjusted so they continuously move particles by increments that are less than the wire spacing. The size of the particle group is broader above the wire, in agreement with the simulation in Fig. 2(b). (b) A group of particles is moved vertically by the matrix over a longer range of five wire spacings. (c) Two groups of particles are moved diagonally to join them together at a single location. Particles can be moved diagonally at any angle. These experimental results agree well with the motion of peaks of the magnetic field magnitude shown in Fig. 2. Current was passed through all 14 wires for the demonstrations shown.

- magnetic particles diameter ~1-2 μm
- superparamagnetic core (the particles are 1–20 nm magnetite nanoparticles coated with a polymer composed of polystyrene and carboxylic acid, suspended in a water based solution.)
- very precise positioning- $\Delta x \approx 10$ μm
- complicated wiring: **free currents produce magnetic field**

Some practical realization of particle transport

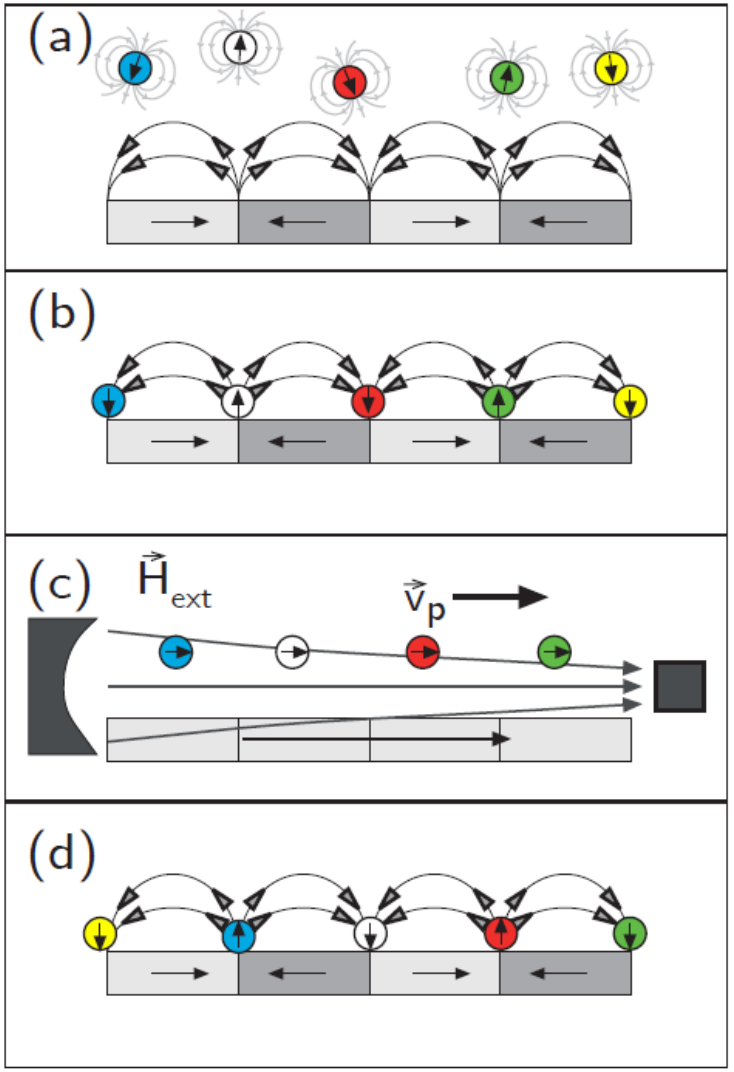

Abb. 5.16: Schematische Darstellung des Konzeptes zum Partikeltransport. (a) Die magnetischen Momente der Partikel richten sich in den Streufeldern der magnetisch strukturierten Probe aus. (b) Die Partikel lagern sich aufgrund der magnetischen Kräfte an den Orten hoher magnetischer Streufelder, d.h. an den Domänenwänden an. (c) Ein externes inhomogenes Magnetfeld sättigt das Substrat und richtet die magnetischen Momente der Partikel neu aus, die dann dem Feldgradienten folgend transportiert werden. (d) Nach Abschalten des externen Feldes lagern sich die Partikel wieder an den Streufeldern der Probe an. Die magnetischen Streufelder der Partikel sind zugunsten der besseren Übersicht nur in (a) eingezeichnet.

Magnetic patterning by 10 keV He^+ bombardment:

change of the exchange bias in **IrMn/NiFe**

Step-wise controllable transport

[8] Tanja Weis, Dissertation, Kassel 2009

Some practical realization of particle transport

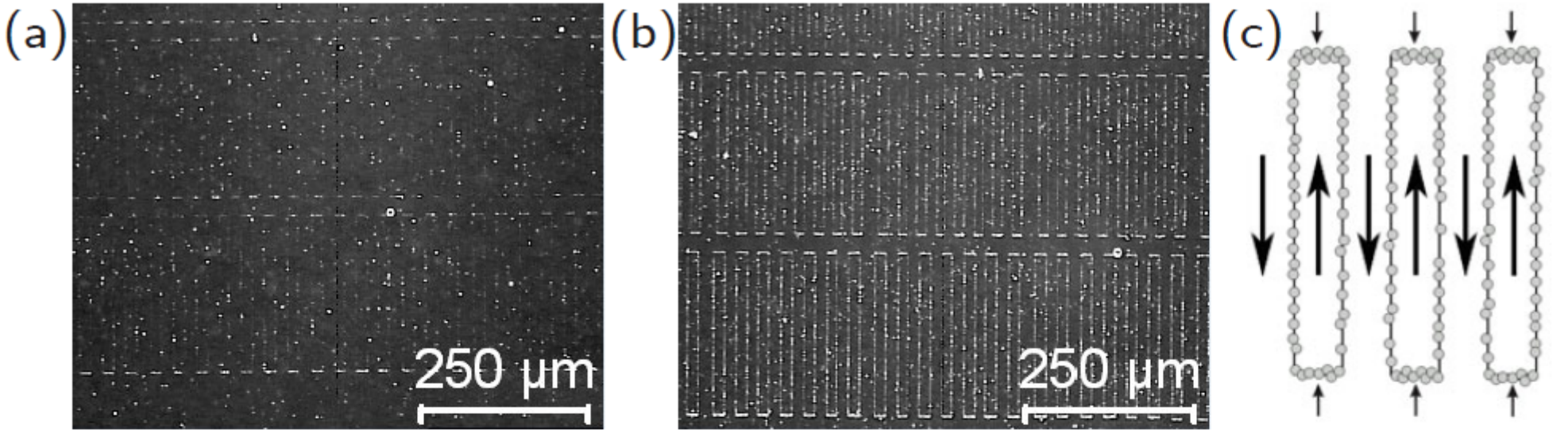

Abb. 5.15: Lichtmikroskopische Aufnahmen von Proben mit magnetischen abgeschlossenen Rechtecken (obere Reihe: 15 μm Breite, 200 μm Länge) nach Aufbringen der 250 nm-Partikel mit der Volumenmethode in Lösung in 100-facher Vergrößerung nach 15 min (a) und nach 60 min (b). Schematische Darstellung der Anlagerung der Partikel an den Domänengrenzen (c). Die Pfeile geben die alternierenden Magnetisierungsrichtungen in den Streifen wieder.

Accumulation of magnetic particles on domain walls

[8] Tanja Weis, Dissertation, Kassel 2009

Colloidal magnetic shift register

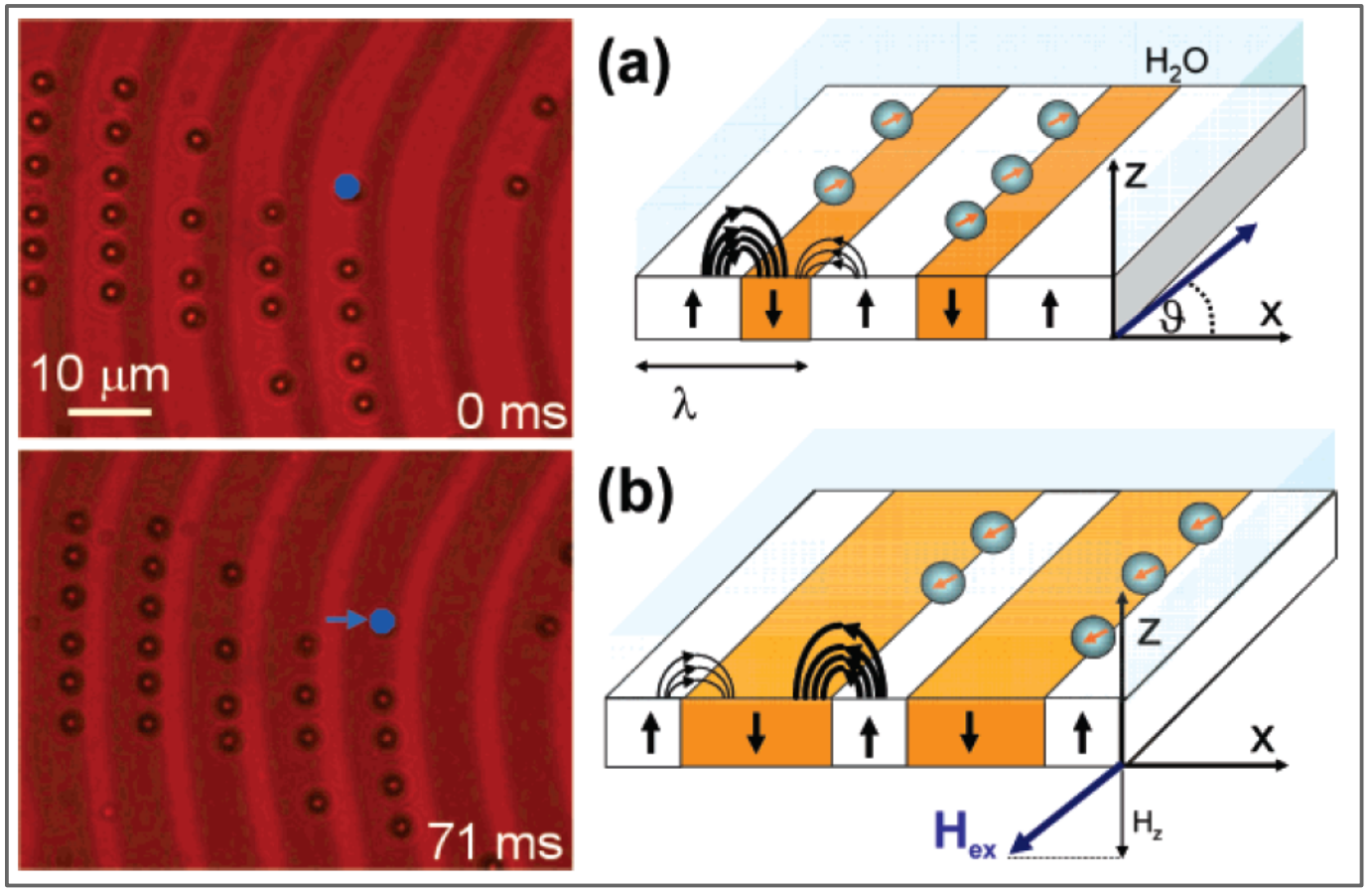

Stripe domain walls stray fields attract magnetic beads placed on the film

λ=10.9 µm

z-component of the external field changes the positions of the domain walls: up and down domains are alternatively wide or narrow

Particles move by **one wavelength in one field cycle**.

- stripe pattern on 5µm thick $Y_{2.5}Bi_{0.5}$ $Fe_{5-q}Ga_qO_{12}$ (q=0.5-1)
- M_S= 17 kA/m
- liquid phase epitaxy
- d= **2.8** µm± 0.1µm; Susceptibility, χ=0.17 (Dynabeads M-270)

[5] Reprinted with permission from P. Tierno, S. V. Reddy, J. Yuan, T. H. Johansen, and T. M. Fischer, J. Phys. Chem. B , 111, 13479 (2007). Copyright 2007 American Chemical Society.

Colloidal magnetic shift register

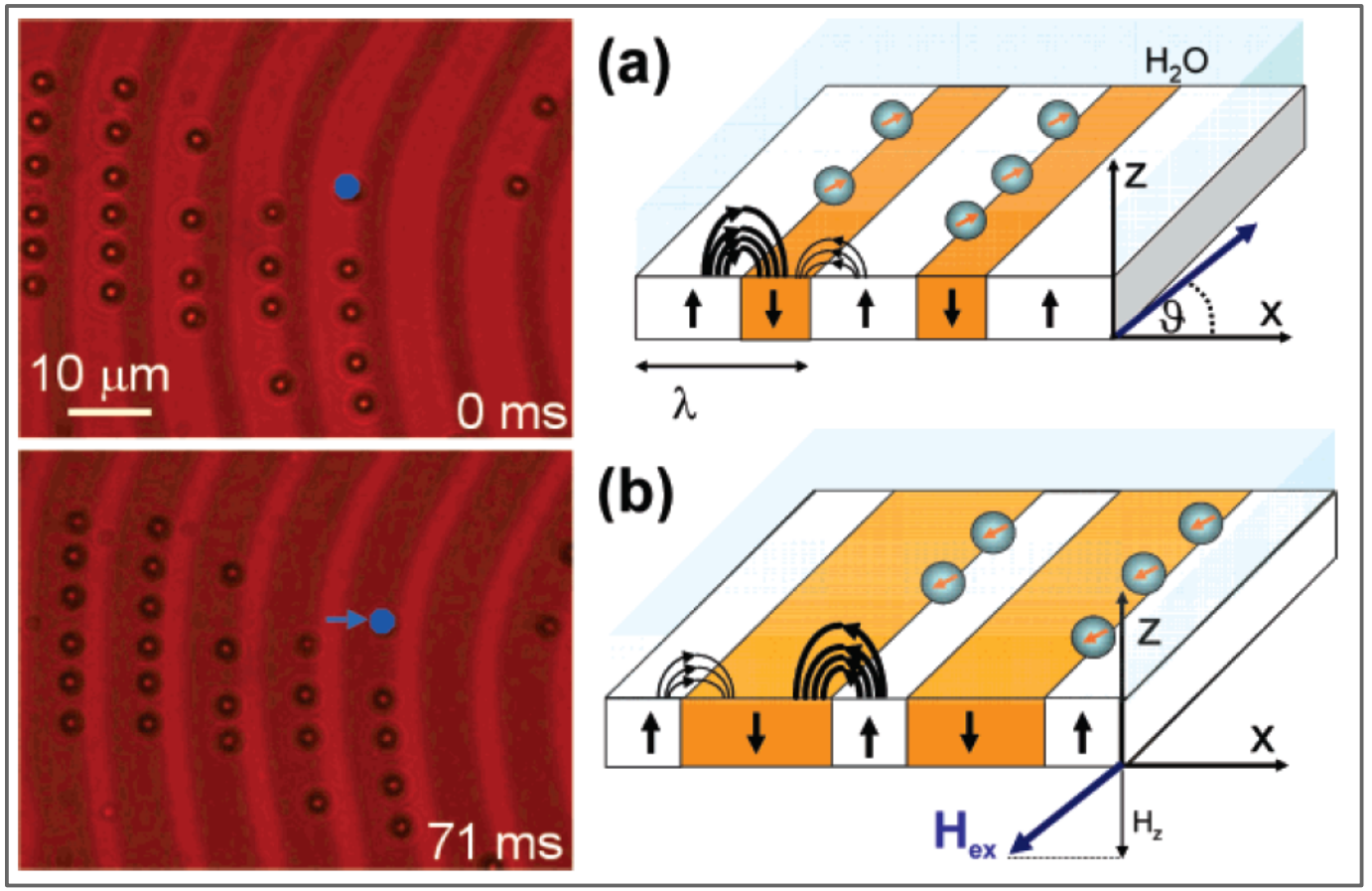

Stripe domain walls stray fields attract magnetic beads placed on the film

λ=10.9 μm

z-component of the external field changes the positions of the domain walls: up and down domains are alternatively wide or narrow

Particles move by **one wavelength in one field cycle**.

$$H_{ext} = 1.3\times10^{4}\left[\vec{i}\sin(\omega t)+\vec{k}\sin(\omega t)\right]\ \text{kA/m}$$

$$6\,s^{-1} < \omega < 125\,s^{-1}$$

$$v_p = \frac{\lambda\,\omega}{2\pi}$$

"Hopping across the domains occurs because the pinning sites alternate between weak and strong during the magnetic modulation of the planar component of the field."

[5] Reprinted with permission from P. Tierno, S. V. Reddy, J. Yuan, T. H. Johansen, and T. M. Fischer, J. Phys. Chem. B , 111, 13479 (2007). Copyright 2007 American Chemical Society.

3D structures - a paternoster for superparamagnetic beads

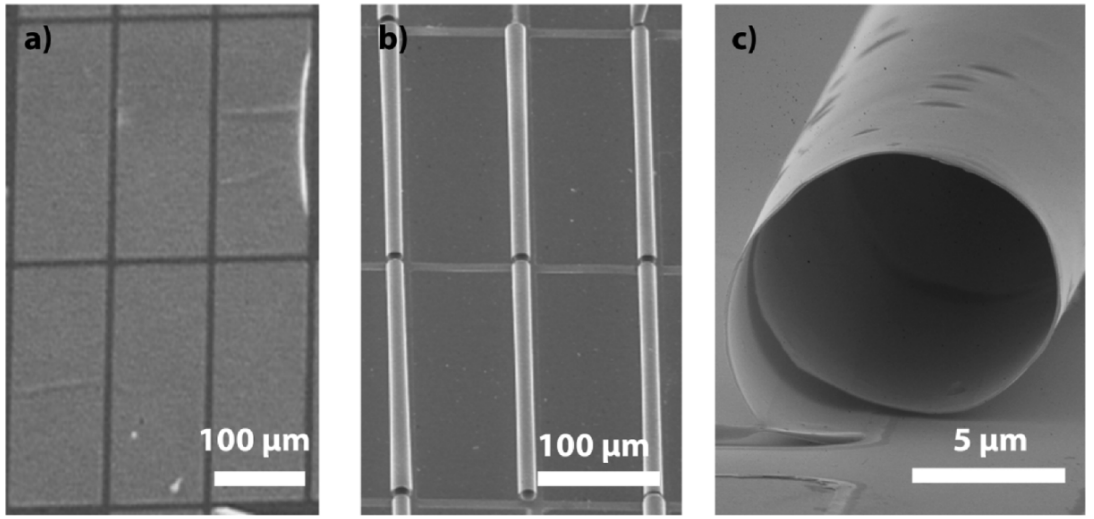

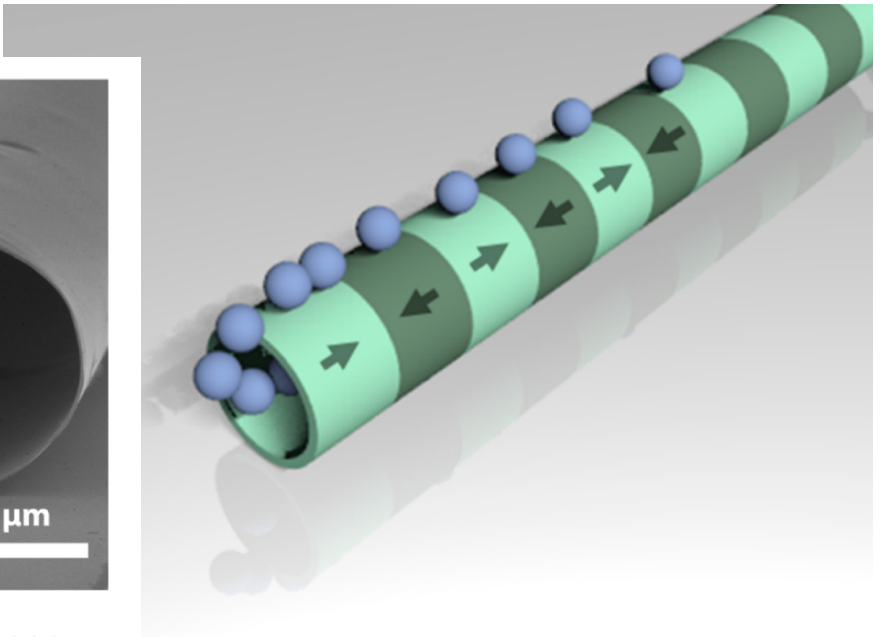

Figure 2. Scanning electron microscopy (SEM) images of 300 × 100 μm^2 sized prestrained layer systems (a) before and (b) after rolling up upon selective release from the substrate. (c) The magnetically stripe patterned exchange bias tubes possess a diameter of about 10 μm.

- exchange bias system: Cu(50nm)/$Ir_{17}Mn_{83}$(10nm)/$Co_{70}Fe_{30}$(7.5nm)/Ta (10nm) deposited via rf sputtering in an external magnetic field of 28 kA/m
- magnetic patterning (the direction of the exchange bias) done with He^+ ion bombardment of the films covered with patterned resist

all the images from T. Ueltzhöffer, R. Streubel, I. Koch, D. Holzinger, D. Makarov, O.G. Schmidt, and A. Ehresmann, ACS Nano **10**, 8491 (2016)

3D structures - a paternoster for superparamagnetic beads

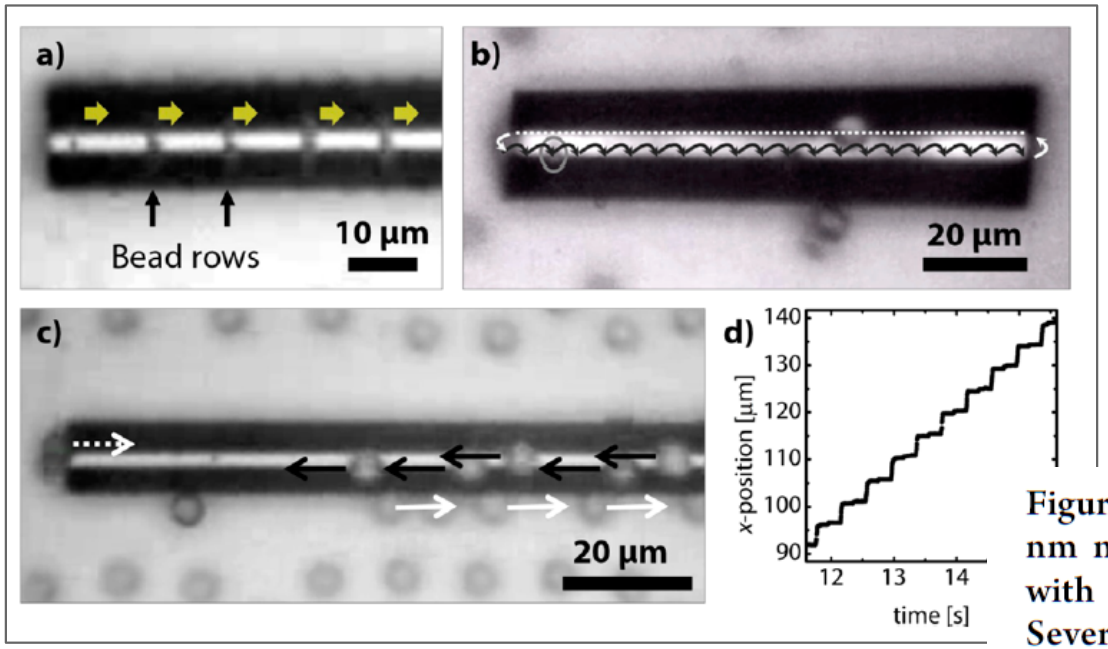

Figure 4. (a) Superparamagnetic beads with diameters of d_1 = 500 nm moving above the magnetically patterned exchange bias tube with a diameter of d_{Tube} = 10 μm (see Supplementary Video 1). Several beads are located close to each other and appear as lines occupying every second domain wall. With each magnetic field pulse of H_z = 5.5 mT, the relevant potential energy minima are shifted to the following domain wall, forcing the beads to move forward. (b) Agglomerate of two superparamagnetic beads each with a diameter of d_2 = 2 μm moving above and retracing inside the magnetically patterned exchange bias tube (see Supplementary Video 2). The black arrows indicate the 20 steps, each from one to another domain wall. The white dotted track indicates the way of retracing inside the tube without changing parameters. (c) Superparamagnetic beads with a diameter of d_3 = 6 μm moving above and next to the magnetically patterned exchange bias tube (see Supplementary Video 3). The direction of transport is reversed at the tube's entrance (white dotted arrow) and next to the tube (white arrows) compared to the one above the tube (black arrows). (d) Step profile of superparamagnetic beads with a diameter of d_2 = 2 μm (recorded from Supplementary Video 2), where the position is depicted versus the time.

the image from T. Ueltzhöffer, R. Streubel, I. Koch, D. Holzinger, D. Makarov, O.G. Schmidt, and A. Ehresmann, ACS Nano **10**, 8491 (2016)

Viscous drag force – Stokes law

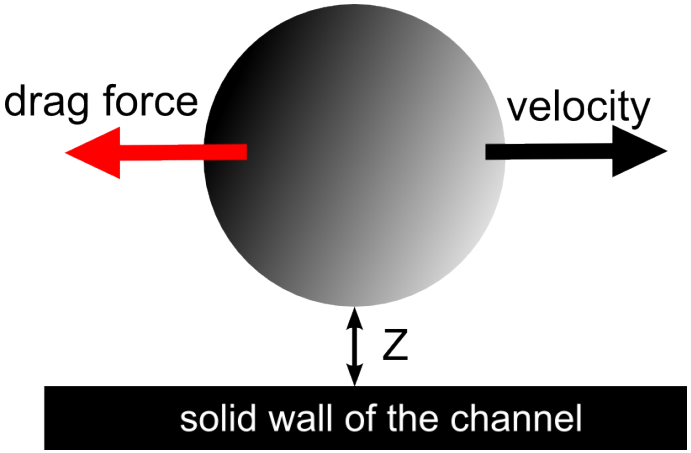

$$F_d = 6\pi\eta r \Delta v f_D$$

$$f_D = \left(1 - \frac{9}{16}\left(\frac{r}{r+z}\right) + \frac{1}{8}\left(\frac{r}{r+z}\right)^3 - \frac{45}{256}\left(\frac{r}{r+z}\right)^4 - \frac{1}{16}\left(\frac{r}{r+z}\right)^5\right)$$

$\eta - viscosity\ (8.9\times10^{-4}\ N\,s\,m^{-2}\ for\ water)$

$f_D - drag\ coefficient$

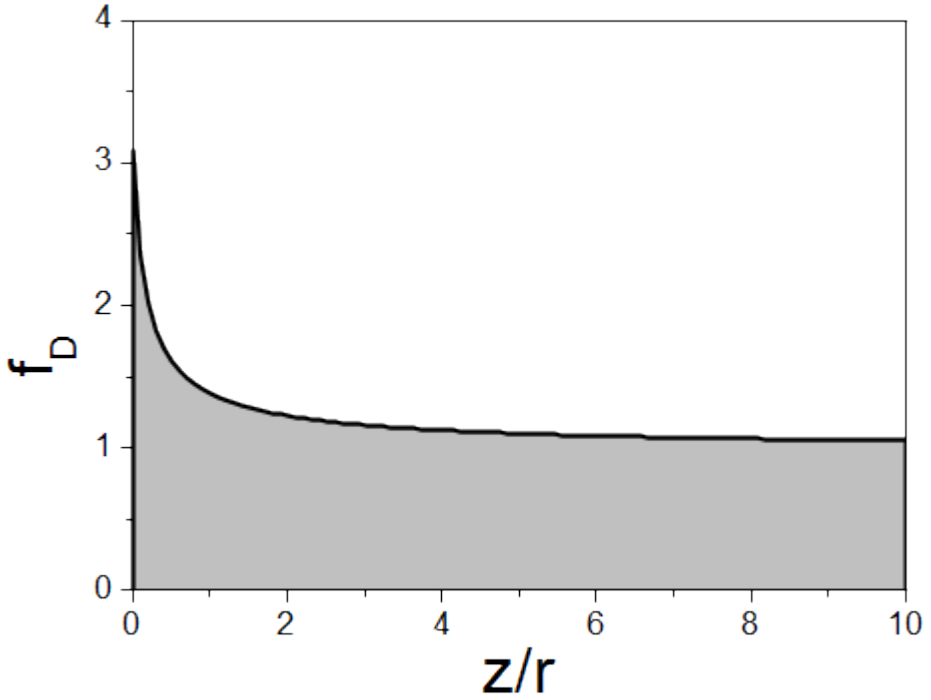

The influence of channel walls is significant for z/r approximately less than 2.

Viscous force is position dependent!

[1] Martin A. M. Gijs, Frédéric Lacharme, and Ulrike Lehmann, Chamical Reviews **110**, 1518 (2010)

Viscous drag force – Stokes law

$$F_d = 6\pi\eta r \Delta v f_D$$

$$f_D = \left(1 - \frac{9}{16}\left(\frac{r}{r+z}\right) + \frac{1}{8}\left(\frac{r}{r+z}\right)^3 - \frac{45}{256}\left(\frac{r}{r+z}\right)^4 - \frac{1}{16}\left(\frac{r}{r+z}\right)^5\right)$$

$\eta - viscosity\ (8.9\times10^{-4}\ N\,s\,m^{-2}\ for\ water)$

$f_D - drag\ coefficient$

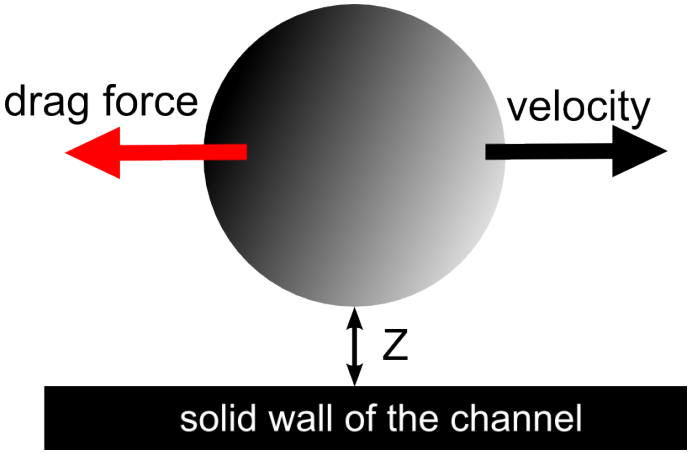

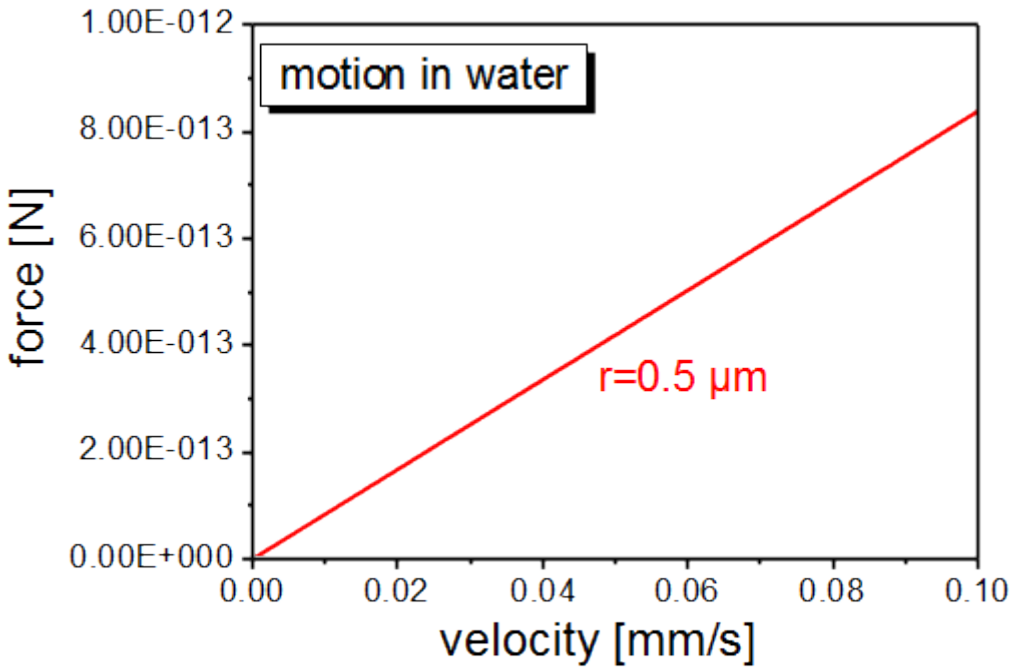

Velocity of the particles in the suspension is limited primarily by the viscous drag.

Viscous drag is approx. proportional to the particle diameter.

[1] Martin A. M. Gijs, Frédéric Lacharme, and Ulrike Lehmann, Chamical Reviews **110**, 1518 (2010)

Sinking speed – gravitation, buoyancy and viscous drag

$$F_d = 6\pi\eta r v \quad f_D = g V (\rho_{bead} - \rho_{fluid})$$

$f_D = 1$

$\eta - viscosity\ (8.9\times10^{-4}\ N\,s\,m^{-2}\ for\ water)$

$f_D - drag\ coefficient$

$\rho_{bead} \approx 1.8\ g/cm^3 \quad (for\ MyOne\ Dynabeads)$

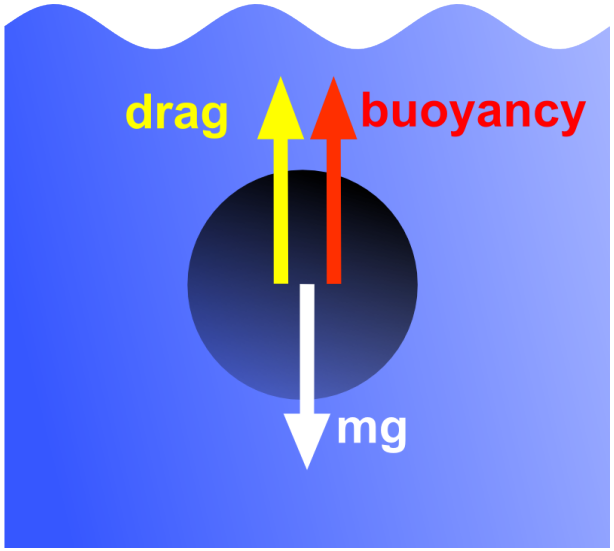

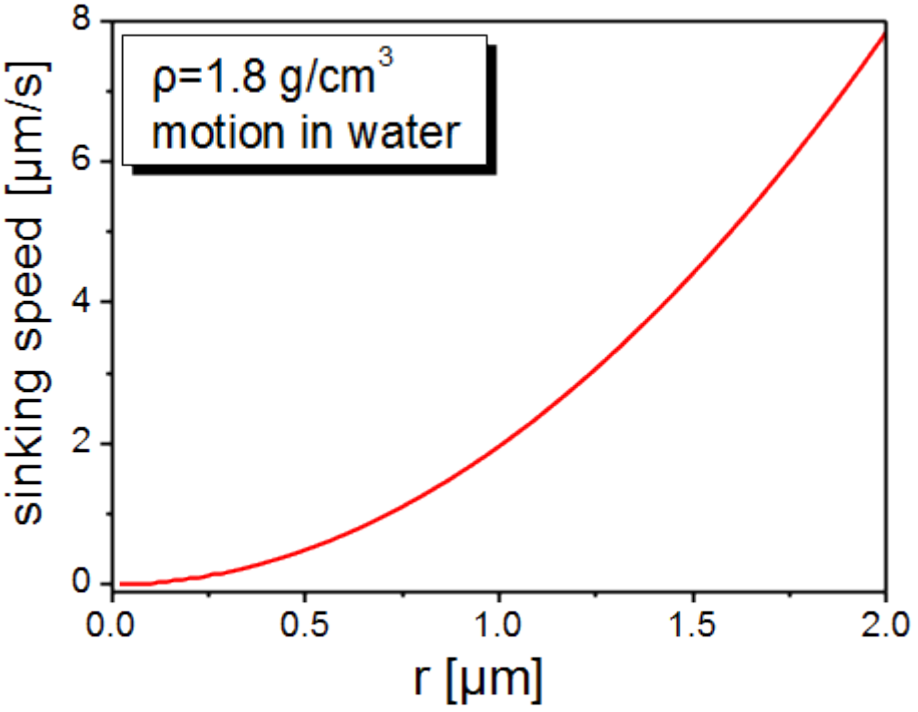

Smaller particles sink much slower

$v_{sink} \sim r^2$

For typical magnetic beads v_{sink} is several μm/s

[1] Martin A. M. Gijs, Frédéric Lacharme, and Ulrike Lehmann, Chamical Reviews **110**, 1518 (2010)

Brownian forces

Stokes-Einstein relation:

$$D = \frac{k_B T}{6 \pi \eta r_{bead}}$$

$D - difussion \;\; coefficient$

$\eta - viscosity \left(8.9 \times 10^{-4} \, N \, s \, m^{-2} \; for \, water \right)$

Mean square displacement of Brownian particle:

$$\left\langle r^2 \right\rangle = 6 D t$$

$t - time$

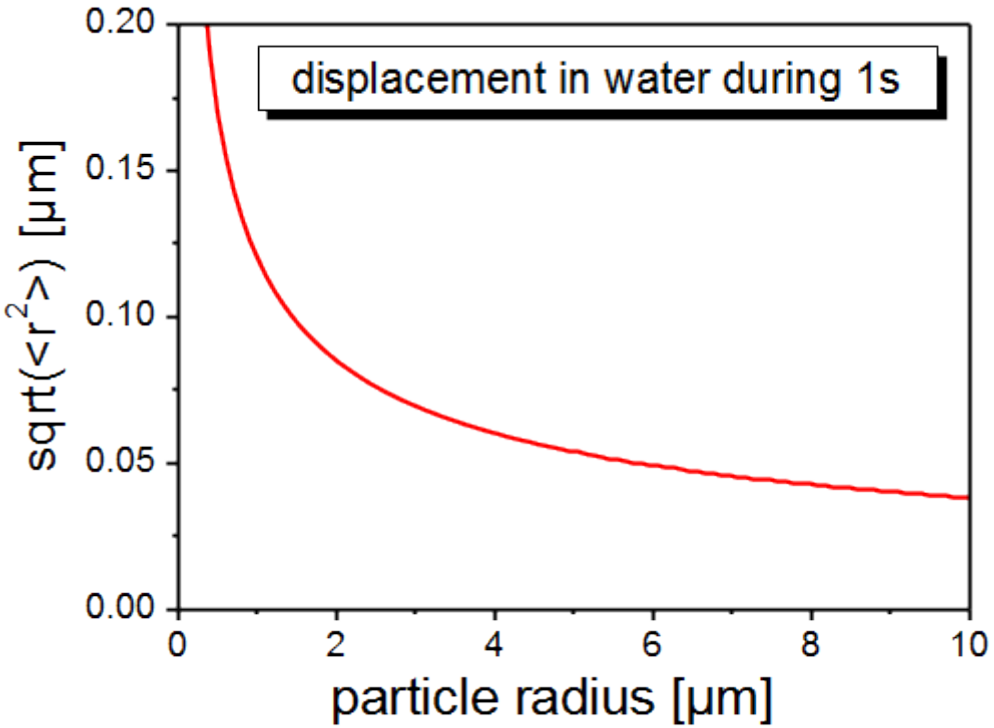

When the magnetic particles are larger than ~1µm the Brownian forces are irrelevant.

sqrt(6*(
1.38*10^(-23)*293/
(6*Pi*x*8.9*10^(-4))
)*1)

[1] Martin A. M. Gijs, Frédéric Lacharme, and Ulrike Lehmann, Chamical Reviews **110**, 1518 (2010)

Steady state velocity

Equation of motion of a particle in a fluid (assuming Stokes viscosity forces)

$$F_{external} = m\frac{d\,x^2}{d\,t^2} + \text{Stokes} \times \frac{d\,x}{d\,t}$$

$$\text{Stokes} = 6\,\pi\,\eta\,r f_D$$

$f_D = 1.5$, η-viscosity ($1.0093 \times 10^{-3}\ N\,s\,m^{-2}$ for distilled water), $\rho_{bead} \approx 1.1\ g/cm^3$

Typical external (magnetic) forces in our system are about 10^{-13} N

$$v(t) = \frac{F_{external}}{\text{Stokes}}\left(1 - e^{-\frac{\text{Stokes} \times t}{m}}\right)$$

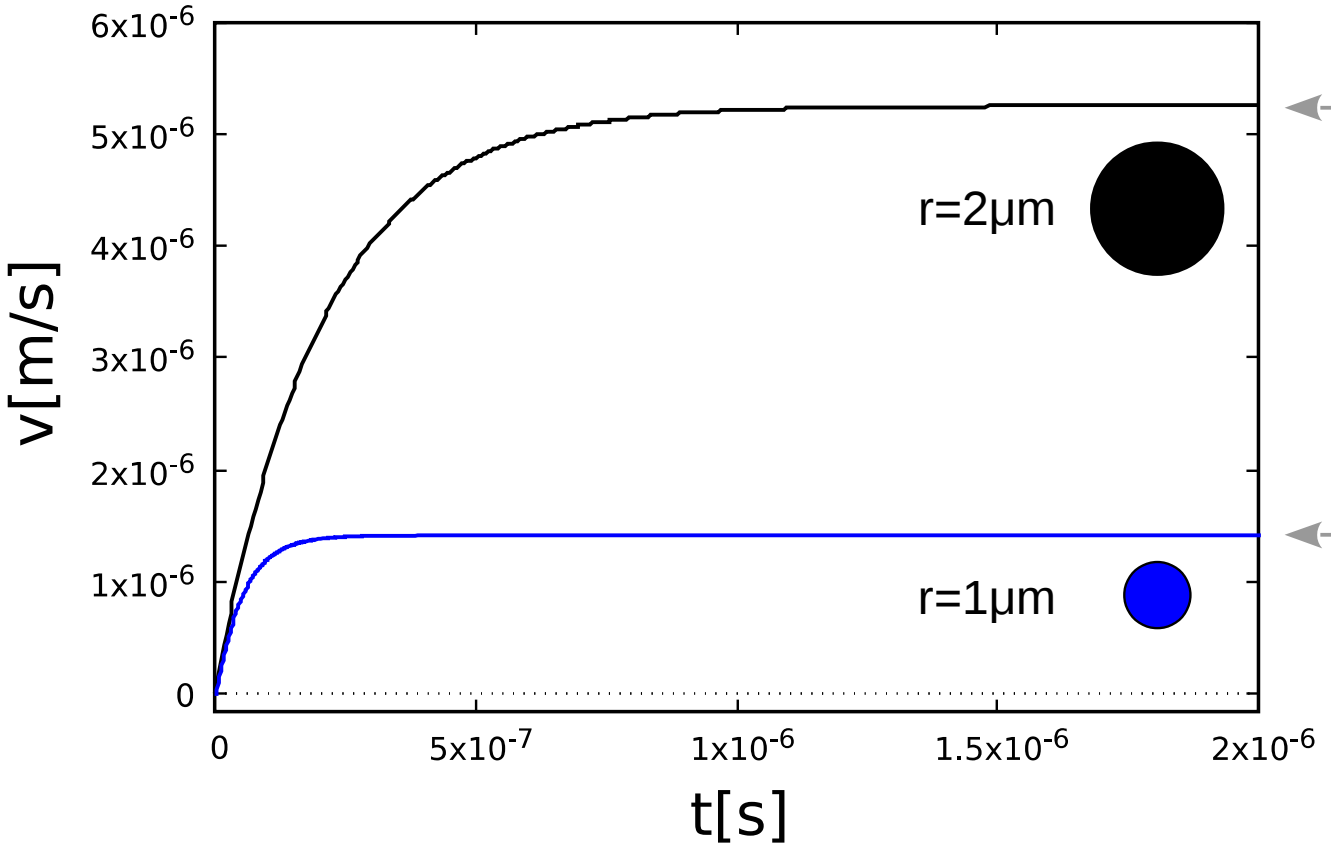

steady state velocity

force assumed proportional to the volume of the bead

Steady state velocity

Equation of motion of a particle in a fluid (assuming Stokes viscosity forces)

$$F_{external} = m\frac{d\,x^2}{d\,t^2} + \text{Stokes} \times \frac{d\,x}{d\,t}$$

$$\text{Stokes} = 6\,\pi\,\eta\,r f_D$$

$f_D = 1.5$, η-viscosity ($1.0093 \times 10^{-3}\ N\,s\,m^{-2}$ for distilled water), $\rho_{bead} \approx 1.1\ g/cm^3$

Typical external (magnetic) forces in our system are about 10^{-13} N

$$v(t) = \frac{F_{external}}{\text{Stokes}}\left(1 - e^{-\frac{\text{Stokes} \times t}{m}}\right)$$

- the beads used in our experiments accelerate to steady state velocity within 1μs
- the distance covered within the acceleration phase in negligible in comparison with characteristic lengths of the experiment (beads diameters, magnetic stripe widths)
- as the external magnetic fields in experiments change with frequencies of the order 0.1-10 Hz it is reasonable to assume that **the beads always move with steady velocities determined by Stokes law**

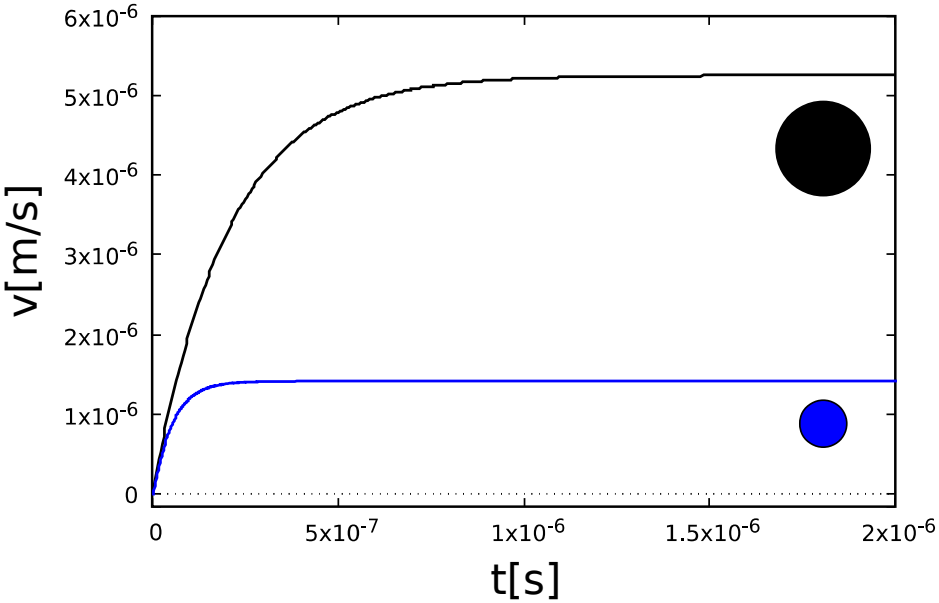

Perpendicular magnetic anisotropy in Au/Co/Au multilayers

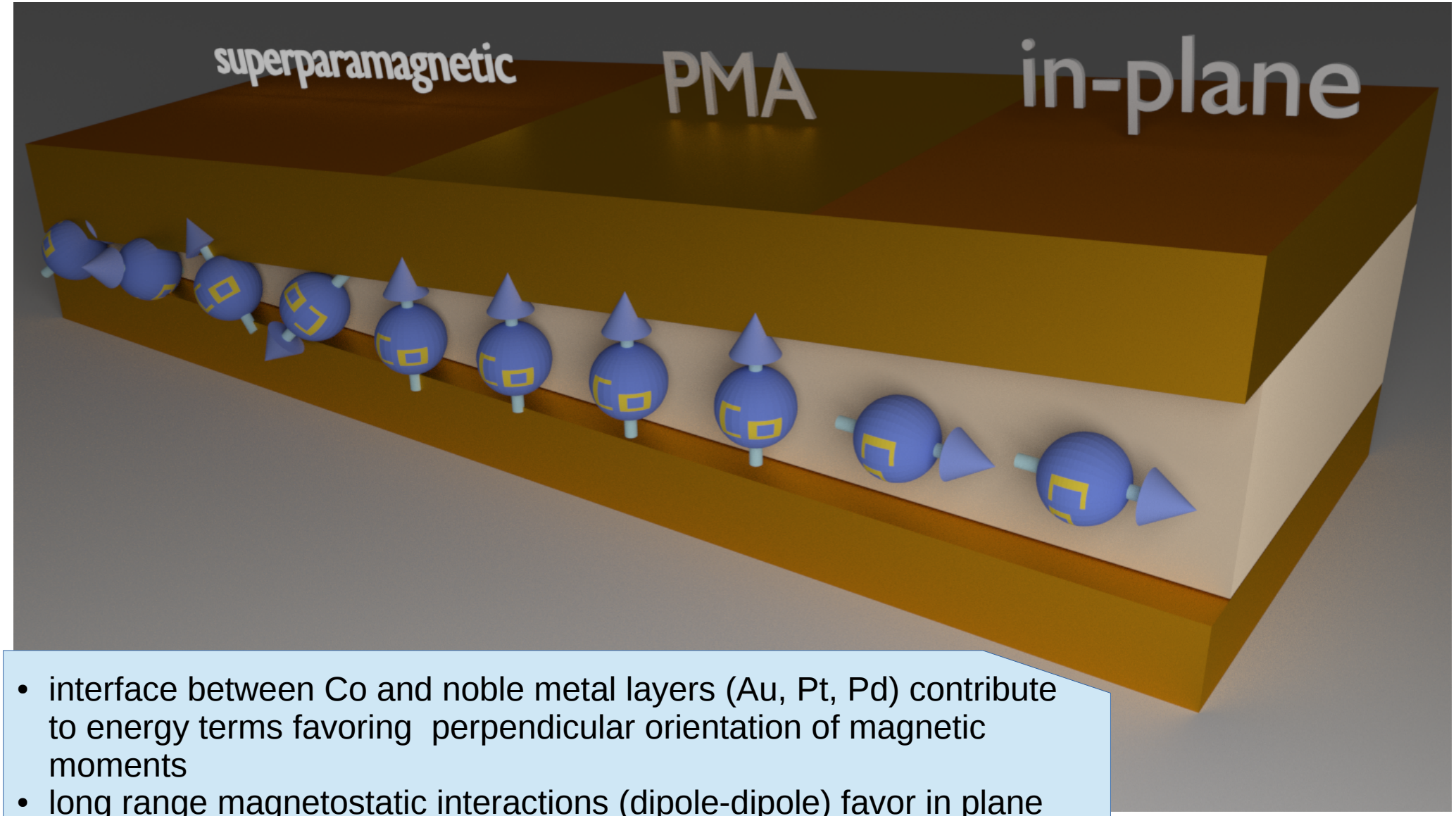

- interface between Co and noble metal layers (Au, Pt, Pd) contribute to energy terms favoring perpendicular orientation of magnetic moments
- long range magnetostatic interactions (dipole-dipole) favor in plane orientation of magnetic moments in thin films
- thin Co films (0.4 -1.5nm) sandwiched between noble metal layers (Au, Pt, Pd) possess perpendicular magnetic anisotropy

Perpendicular magnetic anisotropy in Au/Co/Au multilayers

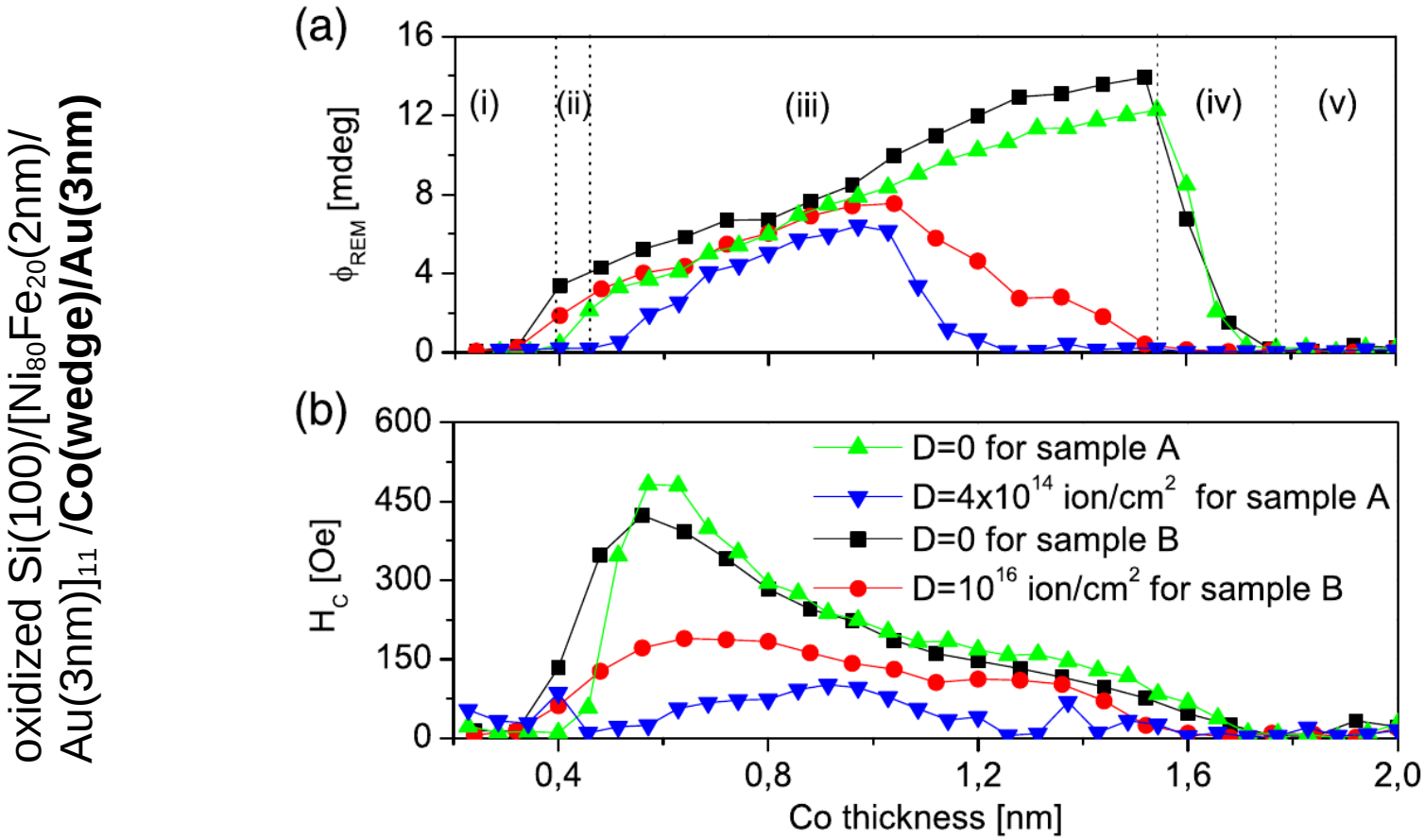

Figure 2. Remnant Kerr rotation ϕ_{REM} (a) and coercive field H_C (b) for a magnetic field H_{ext} applied perpendicular-to-plane for sample A (without mask) and sample B (covered by the colloidal mask) in the as-deposited states and after ion bombardment with different He^+ ion fluences, as functions of the Co layer thickness.

- switching/coercive fields (~35mT) of the Co layers much higher than the fields used in the phoresis experiments (~3mT) – **magnetic moments of Co layers are assumed to be fixed**

Magnetic fields over Au/Co/Au multilayer stripes

- Magnetic field calculated from Biot-Savart law using amperian currents corresponding to magnetization of infinite stripes

$$d\vec{B} = \frac{\mu_0 I}{4\pi} \frac{\hat{dl} \times \vec{r}}{|\vec{r}|^3} \qquad \mu_0 = 4\pi 10^{-7}\,\mathrm{Hm}^{-1}$$

The effect of magnetic moment distribution on magnetic field is the same as that of current distribution given by:

$$\vec{j}_{bound}(\vec{r}) = \nabla \times \vec{M}(\vec{r})$$

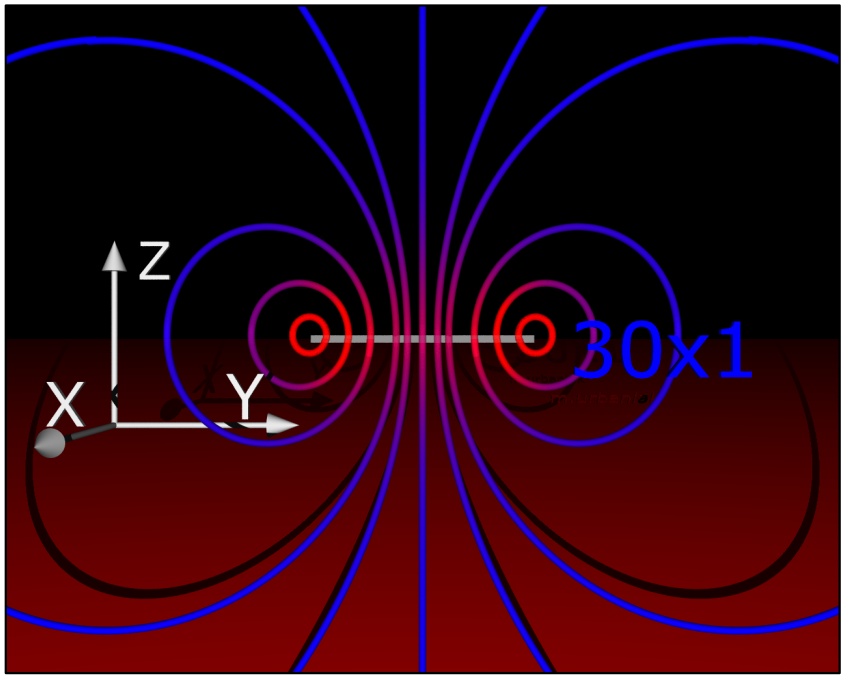

- in thin infinite stripes (aspect ratio > 1000), magnetized perpendicularly to the plane, significant **magnetic fields are present only close to the edges**
- **the fields in the middle of the stripes are negligible**

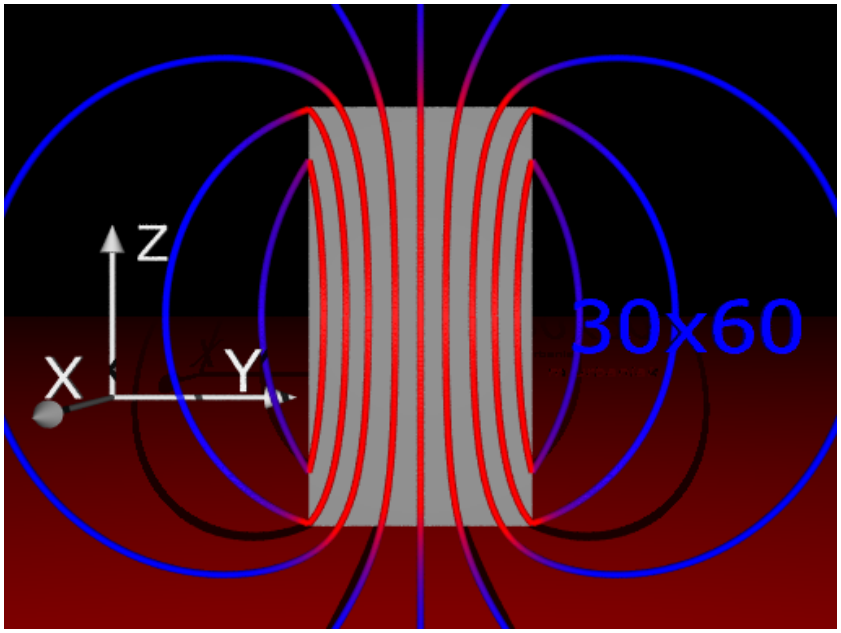

Magnetophoresis

- set of Ti(4 nm)/Au(60 nm)/[**Co(0.7 nm)**/Au(1 nm)]×3 stripes made using electron lithography
- Co layers show the perpendicular magnetic anisotropy
- high switching fields – fixed moments of Co layers

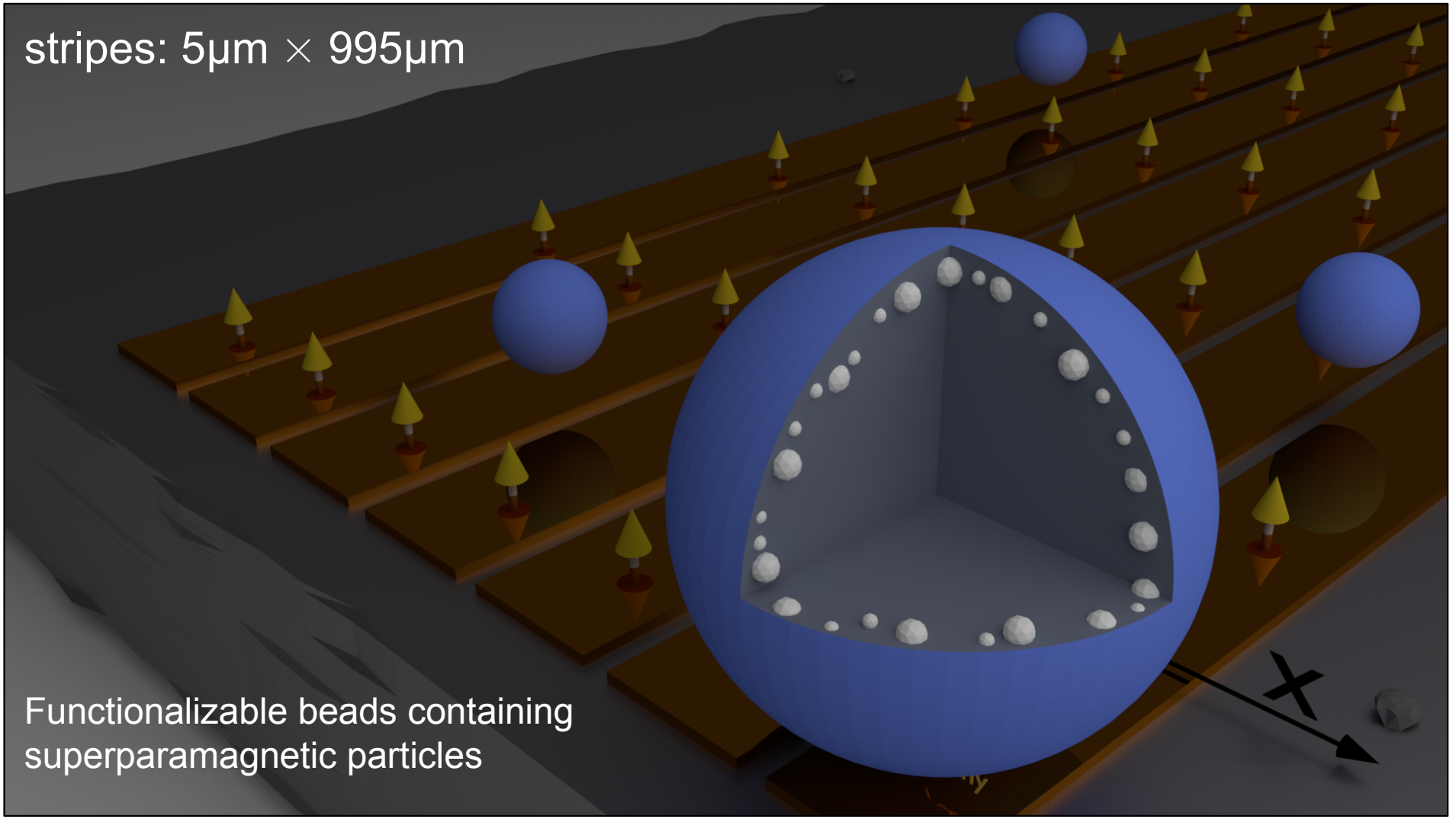

Magnetophoresis

- set of Ti(4 nm)/Au(60 nm)/[**Co(0.7 nm)**/Au(1 nm)]×3 stripes made using electron lithography
- Co layers show the perpendicular magnetic anisotropy
- high switching fields – fixed moments of Co layers

To calculate the force acting on the bead we integrate

$$\vec{F} = \frac{1}{2\mu_0} V \chi_p \nabla B^2$$

over the whole magnetic shell

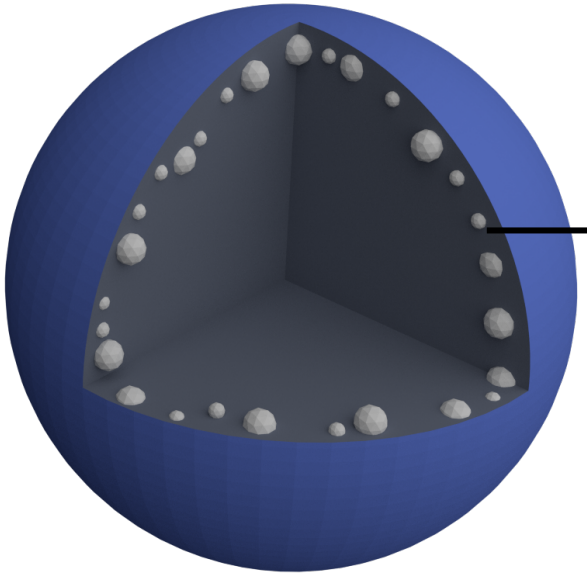

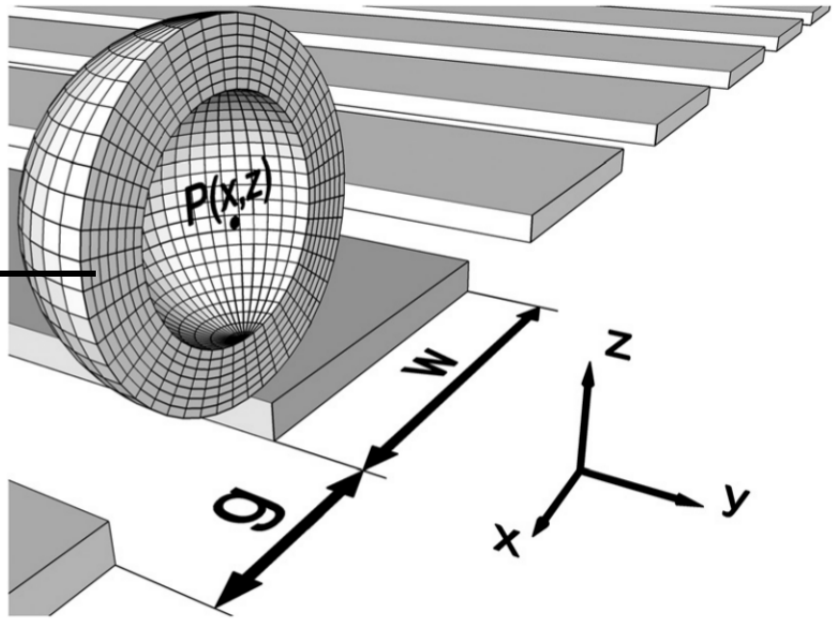

FIG. 5. Schematic drawing of the magnetic bead model used in the calculations. Point P denotes the center of the bead as used in Figs. 6 and 7. Half of the total magnetic volume (the problem is symmetric with respect to the *xz*-plane, containing point *P*) was divided into a number of discretization cells and for each one of them the force components were calculated. The widths of stripes and the widths of gaps are marked as *w* and *g*, respectively. Note that the thicknesses of the stripes and superparamagnetic layer are much exaggerated.

Magnetophoresis – experimental setup

- 2 sets of Helmholtz coils
- stepwise change of magnetic field direction (in plane perpendicular to the stripes)
- switching frequency 0.1 – 10 Hz
- the images were recorded using an Optronics CR450x2 camera with a frame rate of 1000 fps

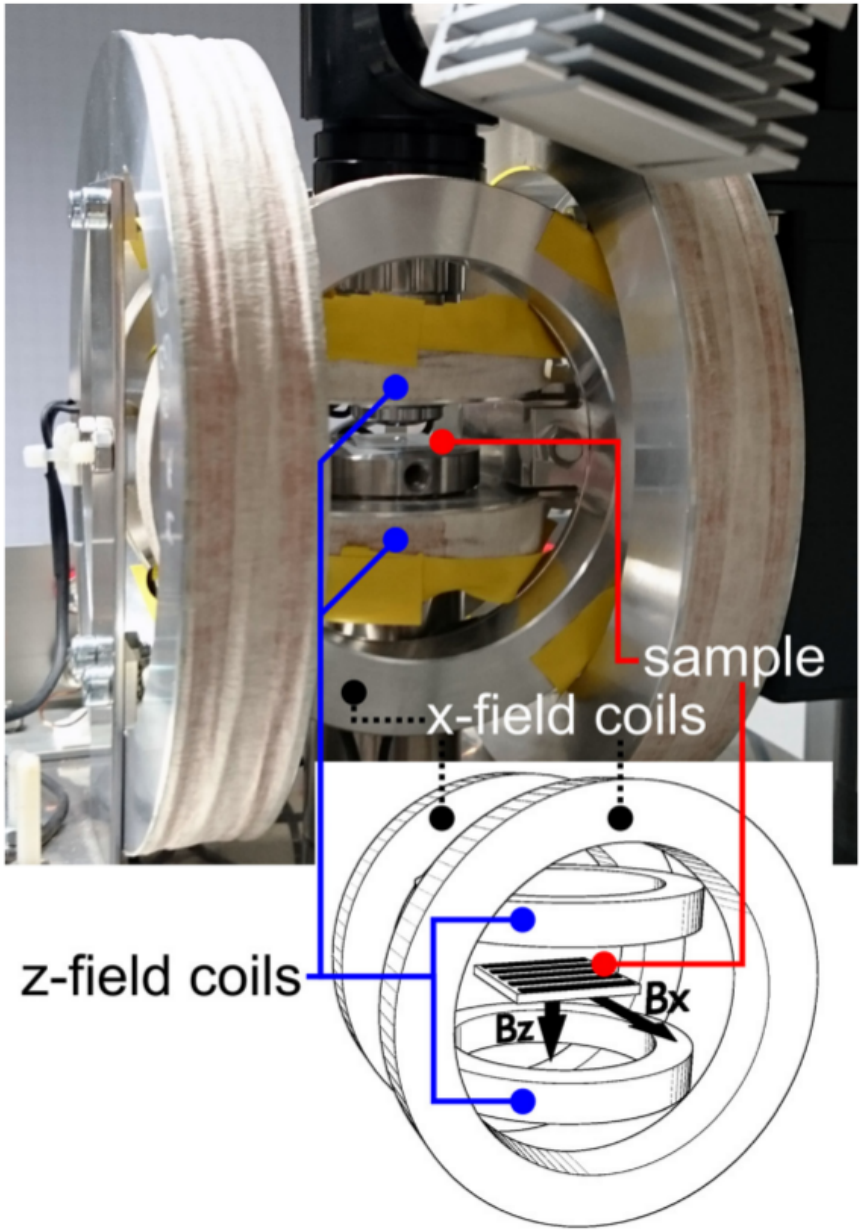

FIG. 2. Photograph of the experimental setup used for the particle transport experiments. The additional sketch shows the orientation of the fields produced by the Helmholtz coils relative to the magnetic stripe structure (shown magnified, black stripes). The outer diameter of *x*-field coils is 94 mm.

Magnetophoresis

- the force acting on the superparamagnetic beads can be calculate using the formula (the formula is true within the field range in which susceptibility is constant)

$$\vec{F}_m = \frac{1}{2\,mu_0} V\,\chi\,\nabla\,\vec{B}^2$$

The field of the stripes creates the energy landscape in which the locations of the beads over the gaps between the stripes are energetically favored

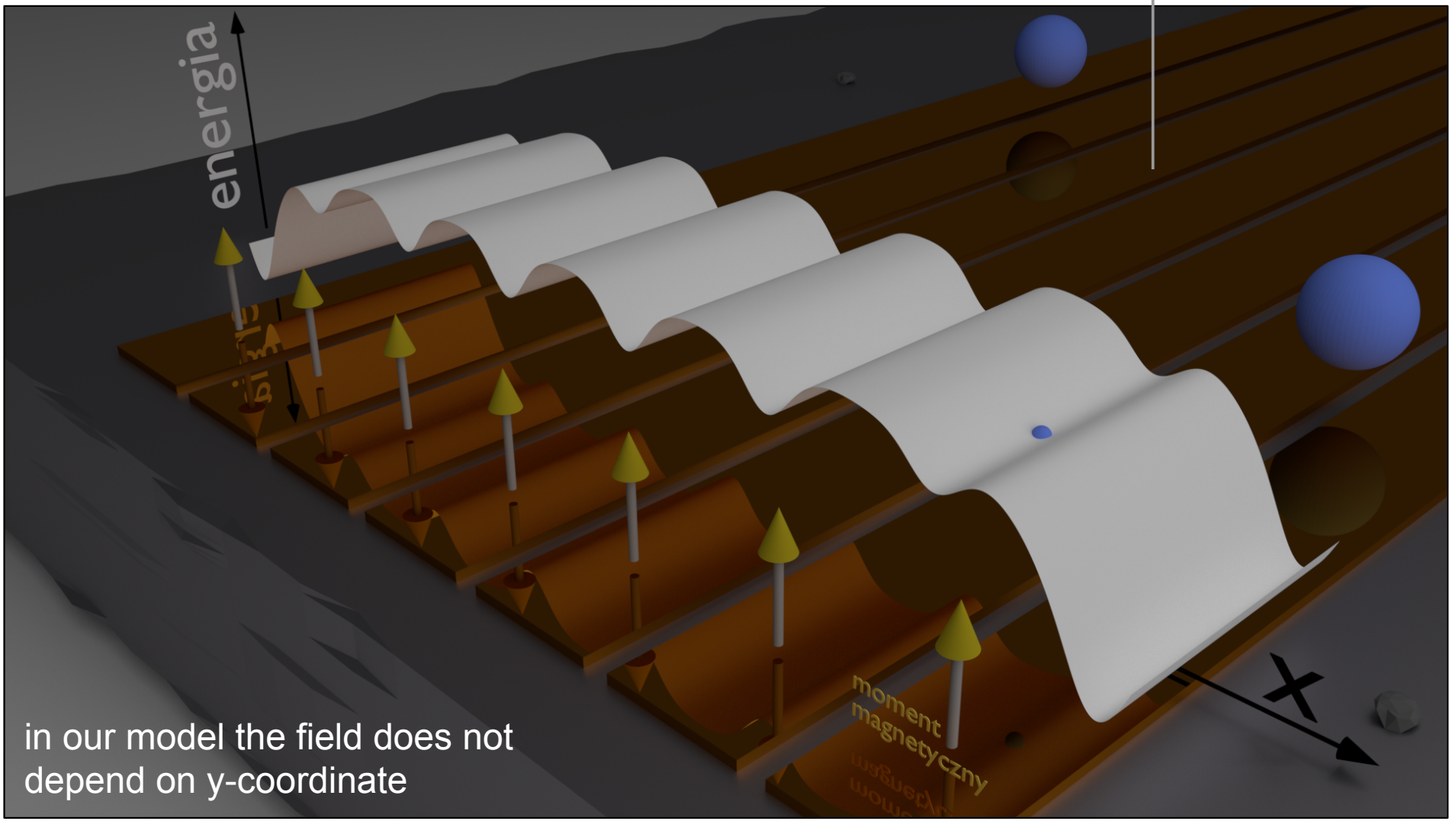

in our model the field does not depend on y-coordinate

Magnetophoresis

- application of the external field can change the positions of the beads corresponding to magnetostatic energy minima
- in the experiment the field is applied in the xz plane ($|B_x|$=1.62mT, $|B_z|$=2.05mT)

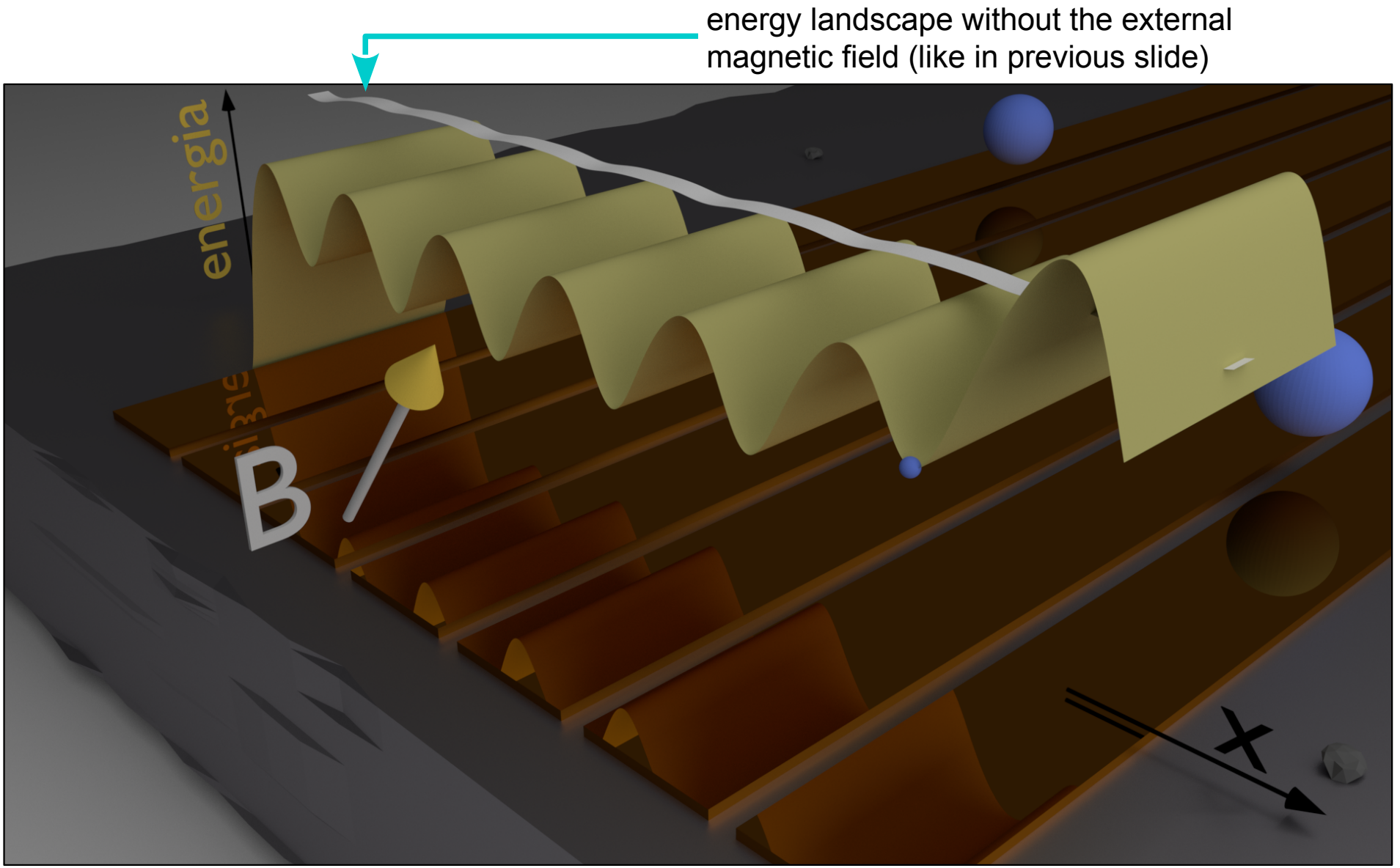

Magnetophoresis

- different configurations of the external field [(+$|B_x|$,+$|B_z|$),(+$|B_x|$,-$|B_z|$), (-$|B_x|$,-$|B_z|$), (-$|B_x|$,+$|B_z|$)] correspond to different equilibrium positions
- a proper sequence of the field configurations leads to a monotonic changes of equilibrium positions

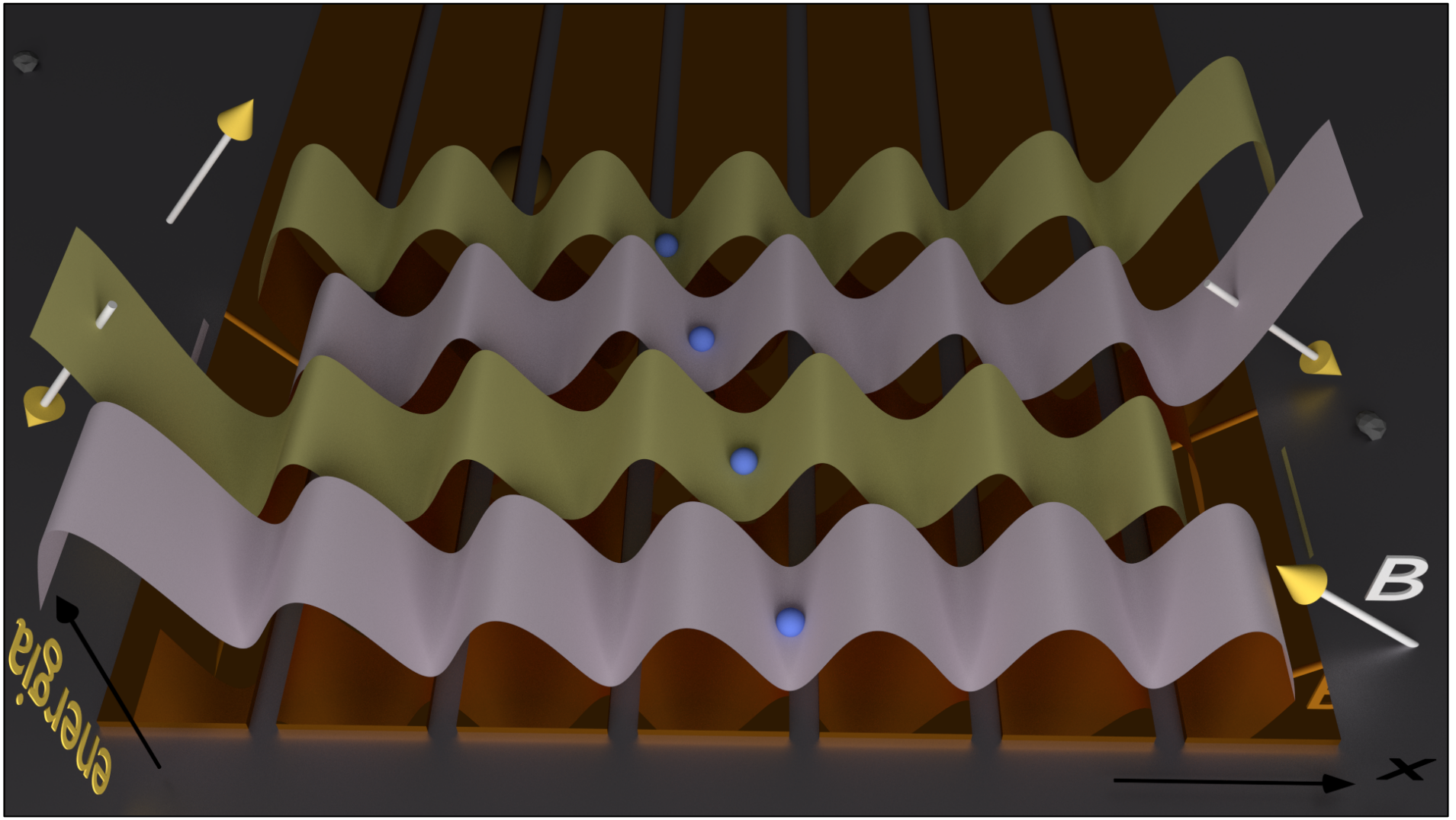

Magnetophoresis

- a proper sequence of the field configurations leads to a monotonic changes of equilibrium positions
- a transition to dependence on time requires taking into account the kind of medium in which the movement occurs – the beads are placed in **water**

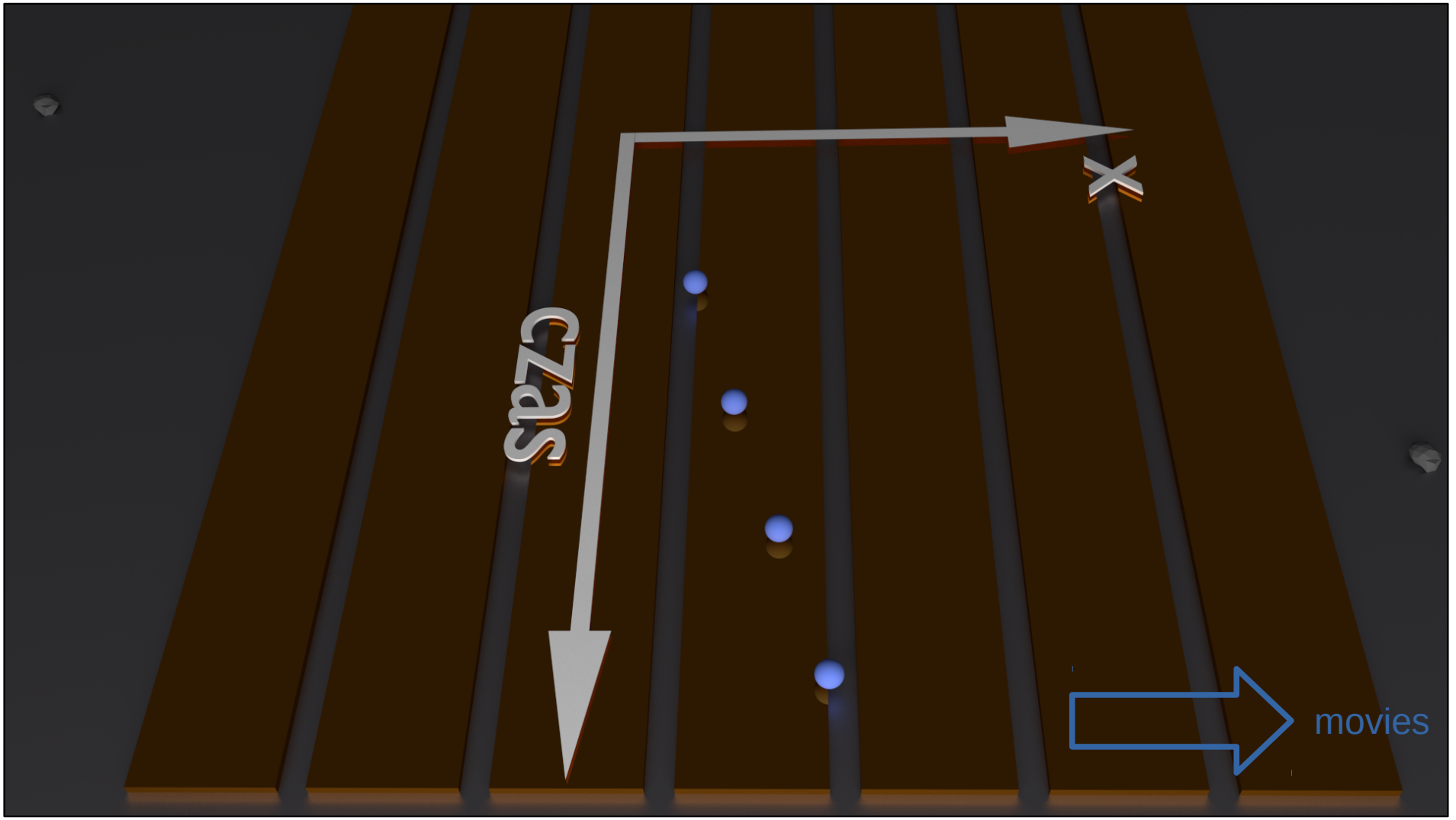

Magnetophoresis

- a proper sequence of the field configurations leads to a monotonic changes of equilibrium positions
- a transition to dependence on time requires taking into account the kine of medium in which the movement occurs – the beads are placed in **water**

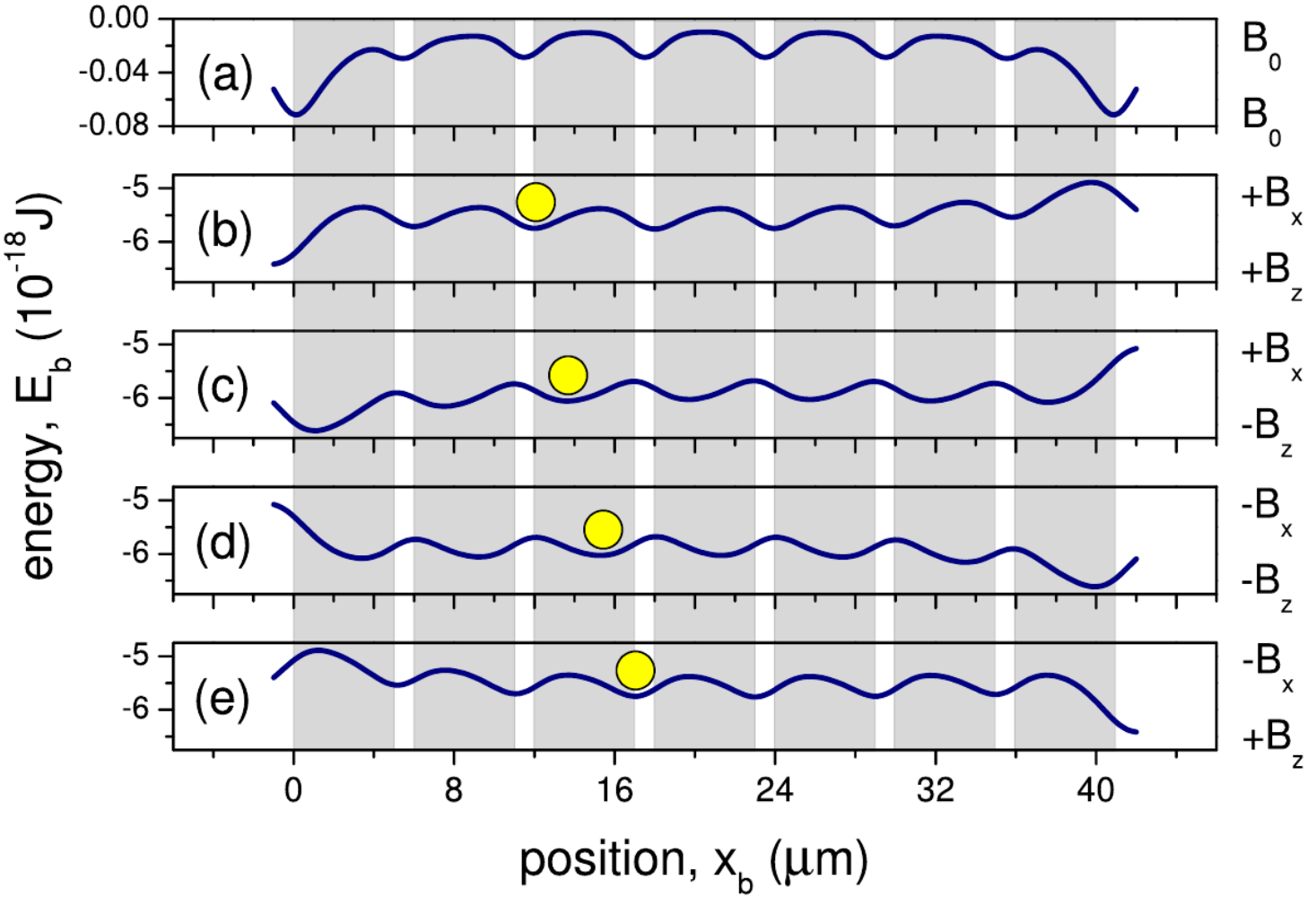

using the Stokes law for a sphere moving in viscous medium we can estimate* the steady state velocities of magnetic beads

$$\vec{F}_m = 6\pi r_b \eta f_R \vec{v}$$

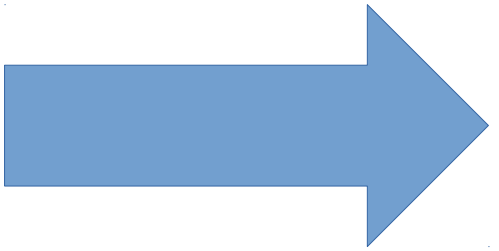

* we do not know the exact distance of the beads from the substrate/magnetic stripes (it is of the order of 500nm → DLVO theory) and we neglect z-component of the magnetic force

Magnetophoresis

- a proper sequence of the field configurations leads to a monotonic changes of equilibrium positions
- a transition to dependence on time requires taking into account the kine of medium in which the movement occurs – the beads are placed in **water**

using the Stokes law for a sphere moving in viscous medium we can estimate* the steady state velocities of magnetic beads

$$\vec{F}_m = 6\pi r_b \eta f_R \vec{v}$$

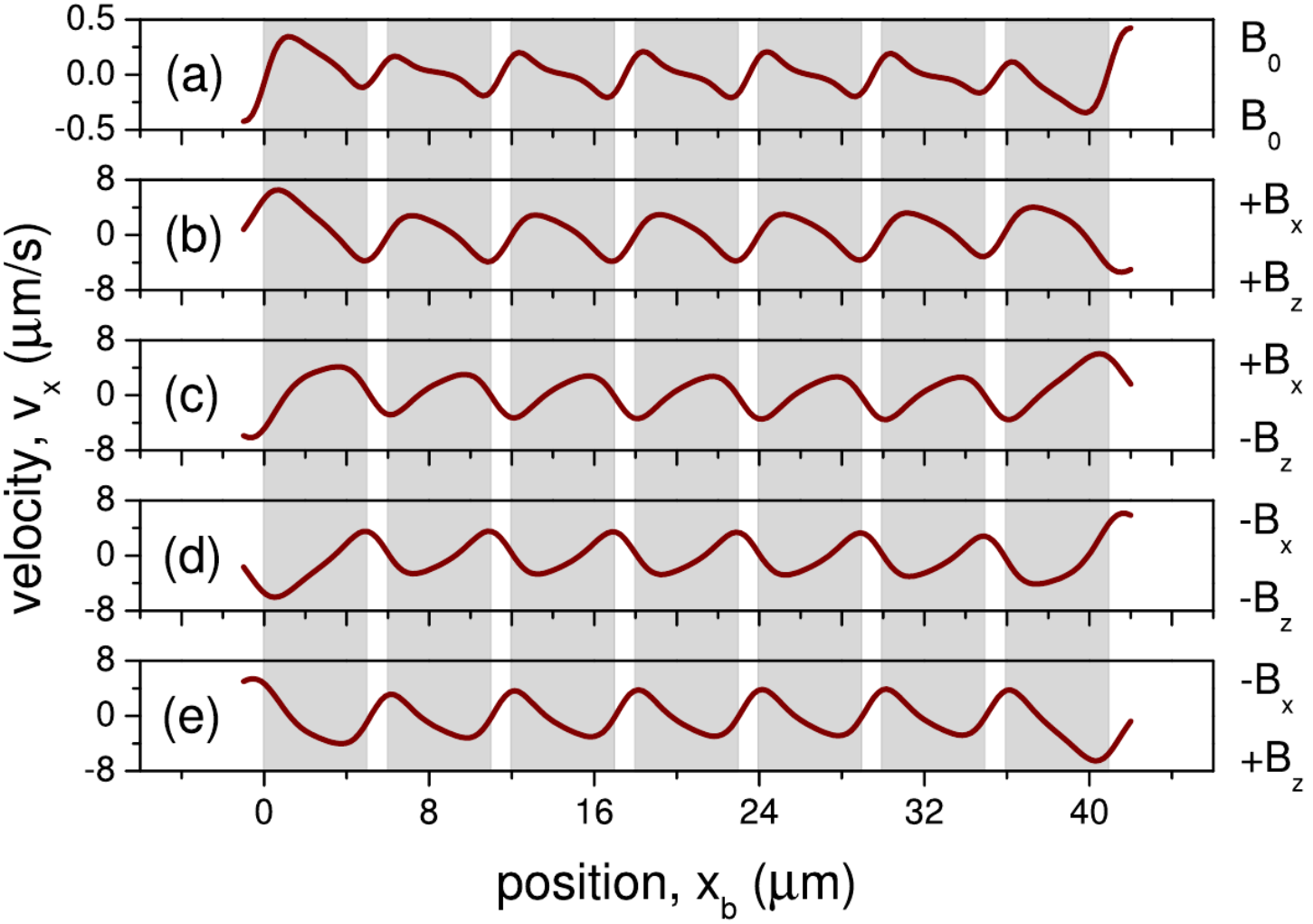

Magnetophoresis

- the velocities of the beads determined using the optical microscopy images are close to those estimated based on calculated magnetic forces

optical microscopy image

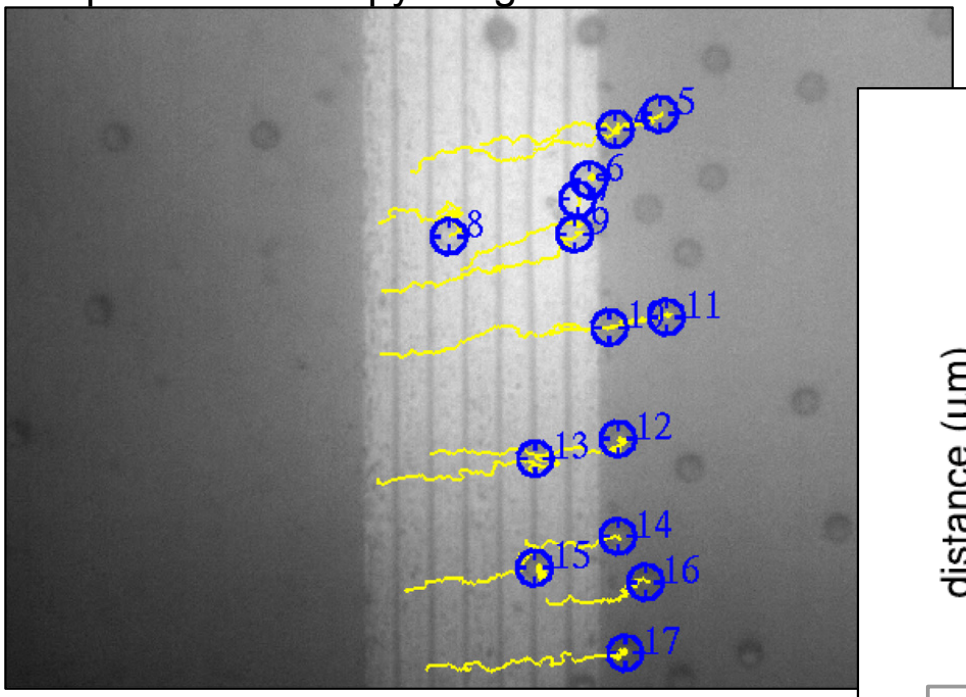

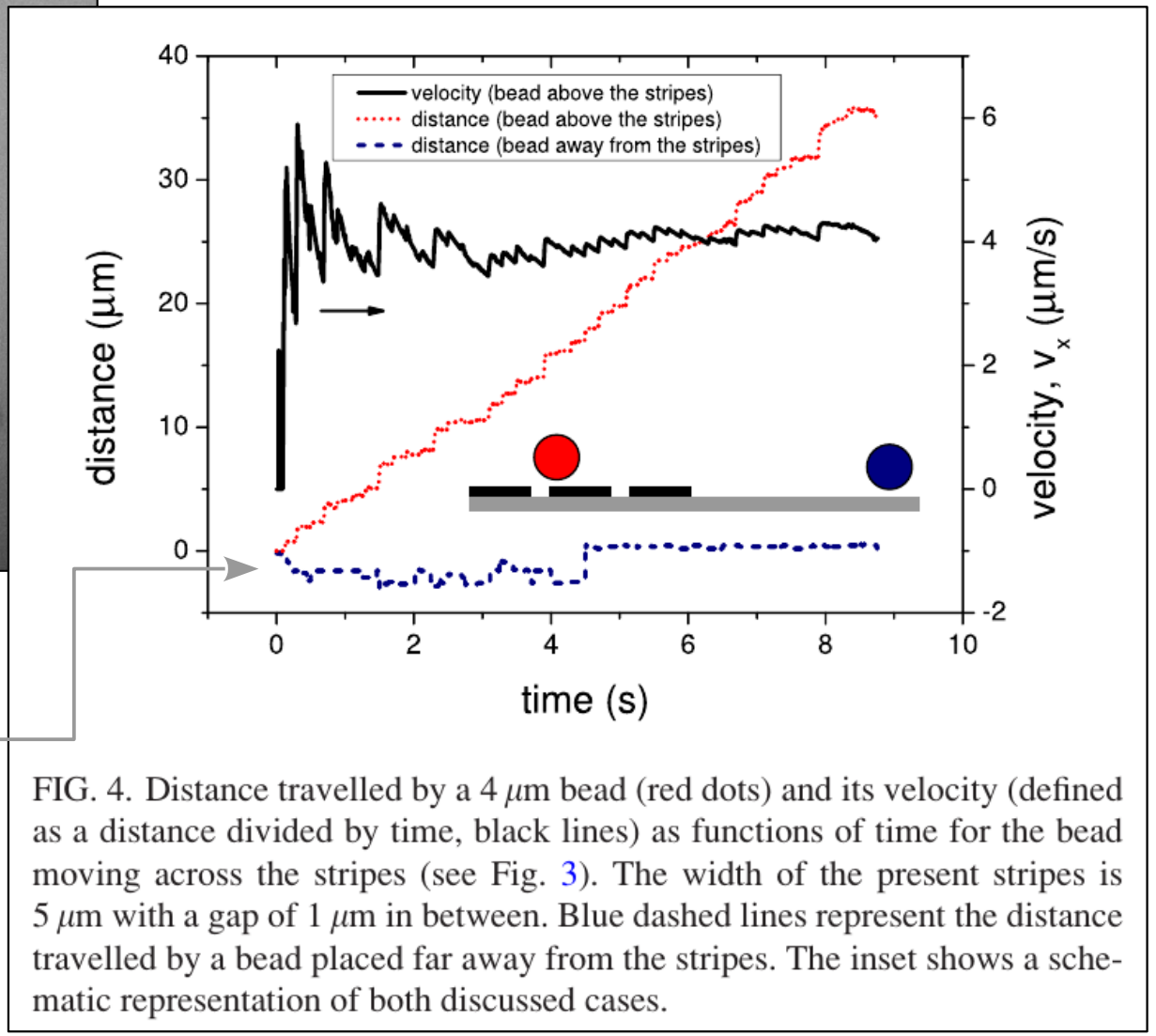

the beads positioned far from the edges of the Au/Co/Au stripes do not perform a steady motion

FIG. 4. Distance travelled by a 4 μm bead (red dots) and its velocity (defined as a distance divided by time, black lines) as functions of time for the bead moving across the stripes (see Fig. 3). The width of the present stripes is 5 μm with a gap of 1 μm in between. Blue dashed lines represent the distance travelled by a bead placed far away from the stripes. The inset shows a schematic representation of both discussed cases.

Magnetophoresis

The model of the motion of the beads allows to:

- determine transport regimes as a function of the frequency of the external magnetic field changes – **if the frequency is to high the beads merely oscillate around the equilibrium position**

- determine the **optimal**, from the point of view of the average velocity, **frequency** of the external magnetic field changes

$$v_x(x,t) = \begin{cases} v_x^c(x), & nT \le t < nT + 0.25\,T \\ v_x^d(x), & nT + 0.25\,T \le t < nT + 0.5\,T \\ v_x^e(x), & nT + 0.5\,T \le t < nT + 0.75\,T \\ v_x^b(x), & nT + 0.75\,T \le t < nT + T, \end{cases}$$

n=1,2,3, …
T- period of magnetic field variations
a,b,c,d relate to the graph shown two slides back

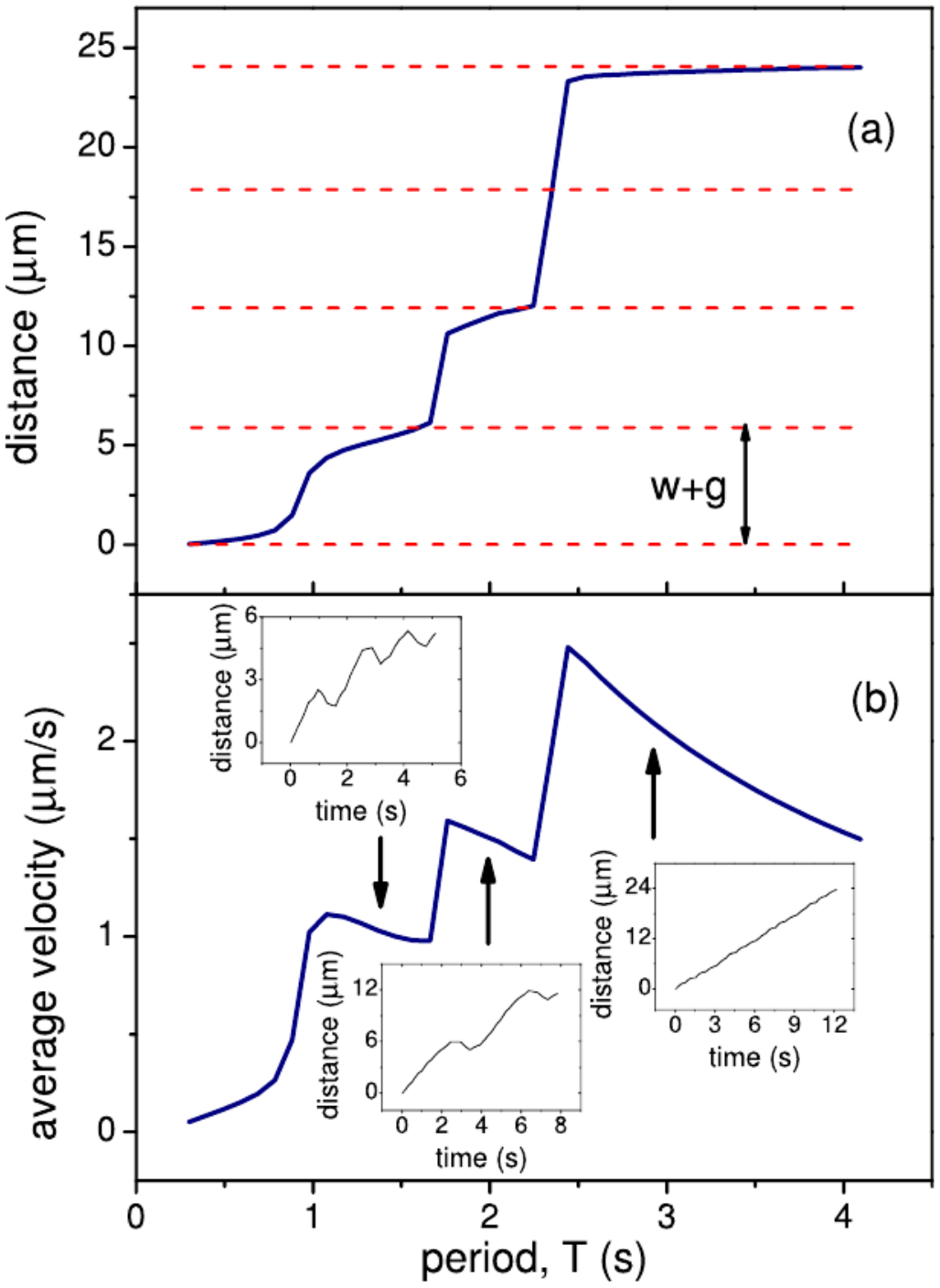

Magnetophoresis

The model of the motion of the beads allows to:

- determine transport regimes as a function of the frequency of the external magnetic field changes – **if the frequency is to high the beads merely oscillate around the equilibrium position**

- determine the **optimal**, from the point of view of the average velocity, **frequency** of the external magnetic field changes

- optimization of the geometry of the system (widths of stripes and gaps for a given diameter of the bead):

$$w \approx g \approx 2r^{*}$$

*for the beads we used – thin magnetic shell of radius r

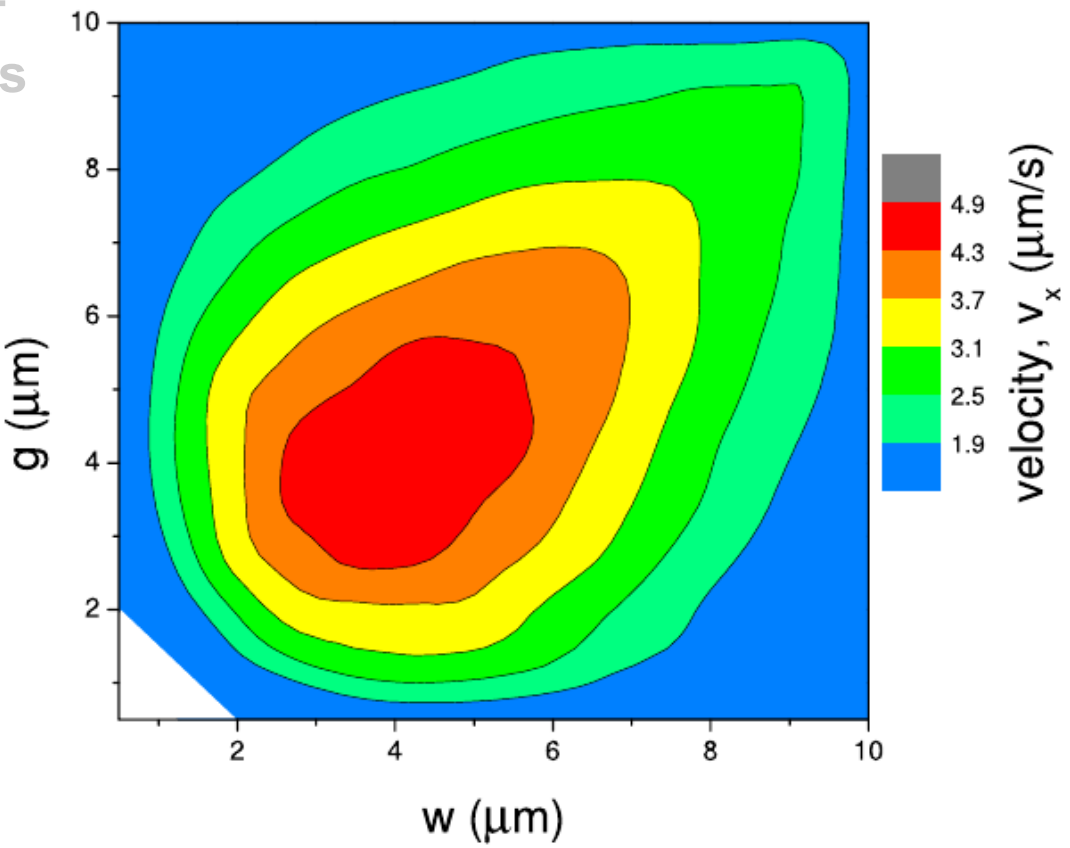

FIG. 9. Map of the maximum average SPB velocity [compare Fig. 7(b)] calculated for different w and g values at $z_b = 2.6$ μm (note that maxima may correspond to different values of T). For g < 2 μm and w < 2 μm (white area) different SPB's movement characteristics are obtained due to deep energy minima at the outer edges of the stripe structure and are therefore not discussed in detail. The map resolution is 0.75 μm.